



THE UNIVERSITY *of* EDINBURGH

Edinburgh Research Explorer

Genomic epidemiology reveals multiple introductions of Zika virus into the United States

Citation for published version:

Grubaugh, ND, Ladner, JT, Kraemer, MUG, Dudas, G, Tan, AL, Gangavarapu, K, Wiley, MR, White, S, Theze, J, Magnani, DM, Prieto, K, Reyes, D, Bingham, A, Paul, LM, Robles-Sikisaka, R, Oliveira, G, Pronty, D, Barcellona, CM, Metsky, HC, Baniecki, ML, Barnes, KG, Chak, B, Freije, CA, Gladden-Young, A, Gnrirke, A, Luo, C, MacInnis, B, Matranga, CB, Park, DJ, Qu, J, Schaffner, SF, Christopher, T-T, West, KL, Winnicki, SM, Wohl, S, Yozwiak, NL, Quick, J, Fauver, JR, Khan, K, Brent, SE, Reiner Jr, RC, Lichtenberger, PN, Ricciardi, M, Bailey, VK, Watkins, DI, Cone, MR, Kopp IV, EW, Hogan, KN, Cannons, AC, Jean, R, Monaghan, AJ, Garry, RF, Loman, NJ, Faria, NR, Porcelli, MC, Vasquez, C, Nagle, ER, Cummings, DAT, Stanek, D, Rambaut, A, Sanchez-Lockhart, M, Sabeti, PC, Gillis, LD, Michael, SF, Bedford, T, Pybus, OG, Isern, S, Palacios, GF & Andersen, KG 2017, 'Genomic epidemiology reveals multiple introductions of Zika virus into the United States', *Nature*, vol. 546, pp. 401–405. <https://doi.org/10.1038/nature22400>

Digital Object Identifier (DOI):

[10.1038/nature22400](https://doi.org/10.1038/nature22400)

Link:

[Link to publication record in Edinburgh Research Explorer](#)

Document Version:

Peer reviewed version

Published In:

Nature

General rights

Copyright for the publications made accessible via the Edinburgh Research Explorer is retained by the author(s) and / or other copyright owners and it is a condition of accessing these publications that users recognise and abide by the legal requirements associated with these rights.

Take down policy

The University of Edinburgh has made every reasonable effort to ensure that Edinburgh Research Explorer content complies with UK legislation. If you believe that the public display of this file breaches copyright please contact openaccess@ed.ac.uk providing details, and we will remove access to the work immediately and investigate your claim.



1 Genomic epidemiology reveals multiple introductions of 2 Zika virus into the United States

3 Nathan D Grubaugh^{1*}, Jason T Ladner^{2,*}, Moritz UG Kraemer^{3,4,5,*}, Gytis Dudas^{6,*}, Amanda L Tan^{7,*},
4 Karthik Gangavarapu^{1*}, Michael R Wiley^{2,*}, Stephen White^{8,*}, Julien Théze^{3,*}, Diogo M Magnani⁹, Karla
5 Prieto², Daniel Reyes², Andrea Bingham¹⁰, Lauren M Paul⁷, Refugio Robles-Sikisaka¹, Glenn Oliveira¹¹,
6 Darryl Pronty⁸, Carolyn M Barcellona⁷, Hayden C Metsky¹², Mary Lynn Baniecki¹², Kayla G Barnes¹²,
7 Bridget Chak¹², Catherine A Freije¹², Adrienne Gladden-Young¹², Andreas Gnirke¹², Cynthia Luo¹²,
8 Bronwyn MacInnis¹², Christian B Matranga¹², Daniel J Park¹², James Qu¹², Stephen F Schaffner¹²,
9 Christopher Tomkins-Tinch¹², Kendra L West¹², Sarah M Winnicki¹², Shirlee Wohl¹², Nathan L
10 Yozwiak¹², Joshua Quick¹³, Joseph R Fauver¹⁴, Kamran Khan^{15,16}, Shannon E Brent¹⁵, Robert C Reiner
11 Jr.¹⁷, Paola N Lichtenberger¹⁸, Michael Ricciardi⁹, Varian K Bailey⁹, David I Watkins⁹, Marshall R
12 Cone¹⁹, Edgar W Kopp IV¹⁹, Kelly N Hogan¹⁹, Andrew C Cannons¹⁹, Reynald Jean²⁰, Andrew J
13 Monaghan²¹, Robert F Garry²², Nicholas J Loman¹³, Nuno R Faria³, Mario C Porcelli²³, Chalmers
14 Vasquez²³, Elyse R Nagle², Derek AT Cummings²⁴, Danielle Stanek¹⁰, Andrew Rambaut^{25,26}, Mariano
15 Sanchez-Lockhart², Pardis C Sabeti^{12,27,28,29#}, Leah D Gillis^{8,#}, Scott F Michael^{7,#}, Trevor Bedford^{16,#},
16 Oliver G Pybus^{3,#}, Sharon Isern^{7,#}, Gustavo Palacios^{2,#,§}, Kristian G Andersen^{1,11,30,#,§}

17
18 ¹Department of Immunology and Microbial Science, The Scripps Research Institute, La Jolla, CA 92037, USA

19 ²Center for Genome Sciences, U.S. Army Medical Research Institute of Infectious Diseases, Fort Detrick, MD 21702, USA

20 ³Department of Zoology, University of Oxford, Oxford OX1 3PS, UK

21 ⁴Boston Children's Hospital, Boston, MA 02115, USA

22 ⁵Harvard Medical School, Boston, MA 02115, USA

23 ⁶Vaccine and Infectious Disease Division, Fred Hutchinson Cancer Research Center, Seattle, WA 98109, USA

24 ⁷Department of Biological Sciences, College of Arts and Sciences, Florida Gulf Coast University, Fort Myers, FL 33965, USA

25 ⁸Bureau of Public Health Laboratories, Division of Disease Control and Health Protection, Florida Department of Health, Miami, FL 33125, USA

26 ⁹Department of Pathology, University of Miami Miller School of Medicine, Miami, FL 33136, USA

27 ¹⁰Bureau of Epidemiology, Division of Disease Control and Health Protection, Florida Department of Health, Tallahassee, FL 32399, USA

28 ¹¹Scripps Translational Science Institute, La Jolla, CA 92037, USA

29 ¹²The Broad Institute of MIT and Harvard, Cambridge, MA 02142, USA

30 ¹³Institute of Microbiology and Infection, University of Birmingham, Birmingham B15 2TT, UK

31 ¹⁴Department of Microbiology, Immunology, and Pathology, Colorado State University, Fort Collins, CO 80523, USA

32 ¹⁵Li Ka Shing Knowledge Institute, St Michael's Hospital, Toronto, ON M5B 1T8, Canada

33 ¹⁶Division of Infectious Diseases, Department of Medicine, University of Toronto, Toronto, ON M5B 1T8, Canada

34 ¹⁷Institute for Health Metrics and Evaluation, University of Washington, Seattle, WA 98121, USA

35 ¹⁸Division of Infectious Diseases, University of Miami Miller School of Medicine, Miami, FL 33155, USA

36 ¹⁹Bureau of Public Health Laboratories, Division of Disease Control and Health Protection, Florida Department of Health, Tampa, FL 33612,

37 USA

38 ²⁰Florida Department of Health in Miami-Dade County, Miami, FL 33125, USA

39 ²¹National Center for Atmospheric Research, Boulder, CO 80307, USA

40 ²²Department of Microbiology and Immunology, Tulane University School of Medicine, New Orleans, LA 70112, USA

41 ²³Miami-Dade County Mosquito Control, Miami, FL 33178 USA

42 ²⁴Department of Biology and Emerging Pathogens Institute, University of Florida, Gainesville, FL 32610, USA

43 ²⁵Institute of Evolutionary Biology, University of Edinburgh, Edinburgh EH9 3FL, UK

44 ²⁶Fogarty International Center, National Institutes of Health, Bethesda, MD 20892, USA

45 ²⁷Center for Systems Biology, Department of Organismic and Evolutionary Biology, Harvard University, Cambridge MA 02138, USA

46 ²⁸Department of Immunology and Infectious Diseases, Harvard T.H. Chan School of Public Health, Harvard University, Boston MA 02115, USA

47 ²⁹Howard Hughes Medical Institute, Chevy Chase, MD 20815, USA

48 ³⁰Department of Integrative Structural and Computational Biology, The Scripps Research Institute, La Jolla, CA 92037, USA

49
50 * = co-first

51 # = co-senior

52 § = co-corresponding

53

54

55

56 **Zika virus (ZIKV) is causing an unprecedented epidemic linked to severe congenital syndromes^{1,2}.**
57 **In July 2016, mosquito-borne ZIKV transmission was reported in the continental United States and**
58 **since then, hundreds of locally-acquired infections have been reported in Florida^{3,4}. To gain insights**
59 **into the timing, source, and likely route(s) of ZIKV introduction, we tracked the virus from its first**
60 **detection in Florida by sequencing ZIKV genomes from infected patients and *Aedes aegypti***
61 **mosquitoes. We show that at least four introductions, but potentially as many as 40, contributed to**
62 **the outbreak in Florida and that local transmission likely started in the spring of 2016 - several**
63 **months before initial detection. By analyzing surveillance and genetic data, we discovered that**
64 **ZIKV moved among transmission zones in Miami. Our analyses show that most introductions are**
65 **linked to the Caribbean, a finding corroborated by the high incidence rates and traffic volumes**
66 **from the region into the Miami area. Our study provides an understanding of how ZIKV initiates**
67 **transmission in new regions.**

68 ZIKV transmission in the Americas was first reported in Brazil in May 2015⁵, though the virus was likely
69 introduced 1-2 years prior to its detection⁶⁻⁸. By January 2016, ZIKV cases were reported from several
70 South and Central American countries and most islands in the Caribbean⁹. Like dengue virus (DENV) and
71 chikungunya virus (CHIKV), ZIKV is vectored primarily by *Aedes* mosquitoes¹⁰⁻¹³. The establishment of
72 the peridomestic species *Ae. aegypti* in the Americas¹⁴ has facilitated DENV, CHIKV, and now likely
73 ZIKV to become endemic in this region¹⁵. In the continental United States, transient outbreaks of DENV
74 and CHIKV have been reported in regions of Texas and Florida^{4,16-21} with abundant seasonal *Ae. aegypti*
75 populations^{14,22}.

76 The 2016 ZIKV outbreak in Florida generated 256 confirmed ZIKV infections⁴ (Fig. 1a). While
77 transmission was confirmed across four counties in Florida (Fig. 1b), the outbreak was most intense in
78 Miami-Dade County (241 infections). Although the case location could not always be determined, at least
79 114 (47%) infections were likely acquired in one of three distinct transmission zones: Wynwood, Miami
80 Beach, and Little River (Fig. 1c-d).

81 Using mosquito surveillance data, we determined the extent of mosquito-borne ZIKV transmission in
82 Miami. Of the 24,351 mosquitoes collected from June to November 2016, 99.8% were *Ae. aegypti* and 8
83 pools of ≤ 50 mosquitoes tested positive for ZIKV (Fig. 1c, Extended Data Fig. 1). From these pools, we
84 estimated that ~ 1 out of 1,600 *Ae. aegypti* mosquitoes were infected (0.061%, 95% CI: 0.028-0.115%,
85 Extended Data Fig. 1a). This is similar to infection rates during DENV and CHIKV outbreaks²³. Although
86 we did not detect ZIKV-infected mosquitoes outside Miami Beach (Fig. 1c), we found that the number of
87 human ZIKV cases correlated strongly with *Ae. aegypti* abundance within each transmission zone
88 (Spearman $r = 0.61$, Fig. 1d, Extended Data Fig. 1b). This suggests that *Ae. aegypti* mosquitoes were the
89 primary mode of transmission and that changes to vector abundance impacted human infection rates. We
90 found that the application of insecticides³ suppressed mosquito populations during periods of intensive
91 usage (Extended Data Fig. 1c), and therefore likely contributed to ZIKV clearance.

92 We sequenced 39 ZIKV genomes from clinical and mosquito samples without cell culture²⁴
93 (Supplementary Table 1a). Our ZIKV dataset included 29 genomes from patients with locally-acquired
94 infections (Fig. 1d) and 7 from *Ae. aegypti* pools (Fig. 1c). We also sequenced 3 ZIKV genomes from
95 travel-associated cases from Florida. Our dataset included cases from all transmission zones in Miami
96 (Fig. 1d) and represented $\sim 11\%$ of all confirmed locally-acquired cases in Florida. We made all sequence
97 data openly available (PRJNA342539, PRJNA356429) immediately after data generation.

98 We reconstructed phylogenetic trees from our ZIKV genomes along with 65 published genomes from
99 other affected regions (Fig. 2, Extended Data Fig. 2 and 3). We found that the Florida ZIKV genomes
100 formed four distinct lineages (labeled F1-F4, Fig. 2a), three of which (F1-F3) belonged to the same clade
101 (labeled A, Fig. 2a). We only sampled a single human case each from the F3 and F4 lineages, consistent

102 with limited transmission (Fig. 2a). The other two Florida lineages (F1-F2) comprised ZIKV genomes
103 from human and mosquito samples within Miami-Dade County (Fig. 2b).

104 Using time-structured phylogenies²⁵, we estimated that at least four separate introductions were
105 responsible for the locally-acquired cases observed in our dataset. The phylogenetic placement of lineage
106 F4 clearly indicates that it resulted from an independent introduction of a lineage distinct from those in
107 clade A (Fig. 2a). For the two well-supported nodes linking lineages F1-F2 (labeled B, Fig. 2a) and F1-F3
108 (A, Fig. 2a), we estimated the time of the most recent common ancestor (tMRCA) to be during the
109 summer of 2015 (95% highest posterior density [HPD]: June-September, 2015). Our data displayed a
110 strong clock signal (Extended Data Fig. 2b) and tMRCA estimates were robust across a range of models
111 (Extended Data Table 1a). Thus while F1-F3 belong to clade A, any fewer than three distinct
112 introductions leading to these lineages would have required undetected transmission of ZIKV in Florida
113 for approximately one year (Fig. 2a).

114 To estimate the likelihood of a single ZIKV transmission chain persisting for over a year, we modeled
115 spread under different assumptions of the basic reproductive number (R_0). Using the number of locally-
116 acquired and travel-associated cases, along with the number of observed genetic lineages, we estimated an
117 R_0 between 0.5 and 0.8 in Miami-Dade County (Extended Data Fig. 4). Even at the upper end of this
118 range, the probability of a single transmission chain persisting for over a year is extremely low (~0.5%,
119 Fig. 2c). This is especially true considering the low *Ae. aegypti* abundance during the winter months
120 (Extended Data Fig. 1d).

121 Given the low probability of long-term persistence, we expect that our ZIKV genomes (F1-F4) were the
122 result of at least four introductions. Differences in surveillance practices and a high number of travel-
123 associated cases (Fig. 1a), however, likely mean that unsampled ZIKV introductions also contributed to
124 the outbreak. To estimate the total number of ZIKV introductions, we modeled scenarios that resulted in
125 241 locally-acquired cases within Miami-Dade County, and found that with R_0 values of 0.5-0.8, we
126 expect 17-42 (95% CI 3-63) separate introductions to have contributed to the outbreak (Fig. 2d). The
127 majority of these introductions would likely have generated a single secondary case that was undetected
128 in our genetic sampling (Extended Data Fig. 4a). Incorporating under-reporting in a sensitivity analysis
129 increases R_0 estimates slightly to 0.7-0.9 (Extended Data Fig. 4f-i).

130 The two main ZIKV lineages, F1 and F2, included the majority of genomes from Florida (92%, Fig. 2a).
131 Assuming they represent two independent introductions, we estimated when each of these lineages
132 arrived in Florida. The probability densities for the tMRCA of both F1 and F2 were centered around
133 March-April, 2016 (Fig. 2b, 95% HPD: January-May, 2016). The estimated timing for these introductions
134 corresponds with suitable *Ae. aegypti* populations in Miami-Dade County²⁶ (Extended Data Fig. 1d) and
135 suggests that ZIKV transmission could have started at least two months prior to its detection in July 2016
136 (Fig. 1a). The dates of the introductions could be more recent if multiple F1 or F2 lineage viruses arrived
137 independently. However, more than 2 introductions would be necessary to substantially change our
138 estimates for the timing of the earliest introduction.

139 To understand transmission dynamics within Miami, we analyzed our genomic data together with case
140 data from the Florida Department of Health (DOH, Supplementary Table 1a). While spatially distinct, the
141 three ZIKV transmission zones occurred within ~5 km of each other (Fig. 1c) and we found that the
142 ZIKV infections associated with each zone overlapped temporally (Fig. 1d). Our ZIKV genomes with
143 zone assignments all belonged to lineages F1 and F2, but neither of these lineages were confined to a
144 single zone (Fig. 2b). In fact, we detected both F1 and F2 lineage viruses from *Ae. aegypti* collected from
145 the same trap 26 days apart (mosquitoes 5 and 8, Fig. 2b). These findings suggest that ZIKV moved
146 among areas of Miami.

147 Determining the sources and routes of ZIKV introductions could help mitigate future outbreaks. We
148 found that lineages F1-F3 clustered with ZIKV genomes sequenced from the Dominican Republic and
149 Guadeloupe (Fig. 2, Extended Data Fig. 2 and 3). In contrast, F4 clustered with genomes from Central
150 America (Fig. 2, Extended Data Fig. 2 and 3). These findings suggest that while ZIKV outbreaks occurred
151 throughout the Americas, the Caribbean islands were the main source of establishing local ZIKV
152 transmission in Florida. Because of severe undersampling of ZIKV genomes, however, we cannot rule out
153 other source areas. Similarly, even though we found that the Florida ZIKV genomes clustered together
154 with sequences from the Dominican Republic, our results do not prove that ZIKV entered Florida from
155 this country.

156 We investigated ZIKV infection rates and travel patterns to corroborate our phylogenetic evidence for
157 Caribbean introductions. We found that the Caribbean islands bore the highest ZIKV incidence rates (Fig.
158 2b), despite Brazil and Colombia reporting the highest absolute number of cases (January to June, 2016,
159 Fig. 3a, Extended Data Fig. 5, Supplementary Table 1b). During the same time period, we estimated that
160 ~3 million travelers arrived from the Caribbean, accounting for 54% of the total traffic into Miami, with
161 the vast majority (~2.4 million) arriving via cruise ships (Fig. 3b, Extended Data Fig. 6, Supplementary
162 Table 1b). Combining the infection rates with travel capacities, we estimated that ~60-70% of ZIKV
163 infected travelers arrived from the Caribbean (Fig. 3c and Extended Data Fig. 7a). We also found that the
164 number of travel-associated ZIKV cases correlated strongly with the expected number of importations
165 from the Caribbean (Spearman $r = 0.8$, Fig. 3d, Extended Data Fig. 7b). Finally, 67% of the travel-
166 associated infections in Florida reported recent travel to the Caribbean (Fig. 3e); however, their mode of
167 travel is unknown. Taken together, these findings suggest that a high incidence of ZIKV in the Caribbean,
168 combined with frequent travel, could have played a key role in the establishment of ZIKV transmission in
169 Florida. These findings, however, do not indicate that cruise ships themselves are risk factors for human
170 ZIKV infection, but only that they served as a major mode of transportation from areas with active
171 transmission. In addition, ZIKV exposure may vary among individuals depending on their purpose of
172 travel and therefore we cannot determine the specific contribution of ZIKV-infected travelers arriving via
173 airlines or cruise ships.

174 The majority of the Florida ZIKV outbreak occurred in Miami-Dade County (Fig. 1b). To determine if
175 there is a higher potential for ZIKV outbreaks in this area, we analyzed incoming passenger traffic from
176 regions with ZIKV transmission along with local *Ae. aegypti* abundance. We estimated that Miami and
177 nearby Fort Lauderdale received ~72% of traffic (Fig. 4) and Miami received more air and sea traffic
178 from ZIKV endemic areas than any other city in the United States (Extended Data Fig. 8). During January
179 to April 2016, we estimated that *Ae. aegypti* abundance was highest in southern Florida²² (Fig. 4,
180 Extended Data Fig. 1d, Extended Data Fig. 8). By June, most of Florida and several cities across the
181 South likely supported high *Ae. aegypti* populations^{14,22} (Extended Data Fig. 8); however, most of this
182 region has not reported local *Ae. aegypti*-borne virus transmission in at least 60 years¹⁹. In fact, the only
183 region outside of Florida with local ZIKV transmission is southern Texas²⁷, which is also the only other
184 region with recent DENV outbreaks¹⁹⁻²¹. Therefore, the combination of travelers, mosquito ecology, and
185 human population density likely make Miami one of the few places in the continental United States at risk
186 for *Ae. aegypti*-borne virus outbreaks^{22,26,28}.

187 The extent of ZIKV transmission in Florida was unprecedented, with more reported ZIKV cases in 2016
188 (256) than DENV cases since 2009 (136)^{4,16,17}. This case difference may be reflected by lower incidence
189 of endemic DENV than epidemic ZIKV in source countries^{29,30}, resulting in fewer DENV importations
190 (reported travel cases since 2009: 654 DENV and 1,016 ZIKV)⁴. Given that the majority of ZIKV
191 infections are asymptomatic^{2,31}, the true number of ZIKV cases was likely much higher. Despite this, we
192 estimated that the average R_0 was less than 1 and therefore multiple introductions were necessary to give
193 rise to the observed outbreak³². The high volume of traffic entering Florida from ZIKV-affected regions,
194 especially the Caribbean, likely provided a substantial supply of ZIKV-infected individuals³³. Because

195 Florida is unlikely to sustain long-term ZIKV transmission³², the potential for future ZIKV outbreaks in
196 this region is dependent upon activity elsewhere. Therefore, we expect that outbreaks in Florida will cycle
197 with the ZIKV transmission dynamics in the Americas^{7,8,15}.

198

199

200

201

202 **Acknowledgements**

203 We thank J. Weger-Lucarelli, G. Ebel, C. Moore, B. Alto, G. Donatti, and S. Taylor for discussions, E.
204 Spencer for IRB and logistics support, M. Pilcher for sequencing assistance, and G. Schroth and S. Gross
205 for designing and providing enrichment probes. N.D.G. is supported by NIH training grant
206 5T32AI007244-33. G.D. is supported by the Mahan Postdoctoral Fellowship from the Computational
207 Biology Program at Fred Hutch. K.G.B. is supported by the ASTMH Shope Fellowship. N.R.F. is funded
208 by a Sir Henry Dale Fellowship (Wellcome Trust/Royal Society Grant 204311/Z/16/Z). D.A.T.C. was
209 supported by US NIH MIDAS program (U54-GM088491) and CDC Cooperative Agreement
210 U01CK000510. A.R. is supported by EU Seventh Framework Programme (FP7/2007-2013) under Grant
211 278433-PREDEMICS, ERC Grant 260864, Horizon 2020 Grant 643476-COMPARE. T.B. is a Pew
212 Biomedical Scholar and is supported by NIH R35 GM119774-01. O.G.P. received funding from EU ERC
213 Seventh Framework Programme (FP7/2007-2013)/ERC number 614725-PATHPHYLODYN and the
214 USAID Emerging Pandemic Threats Program-2 PREDICT-2 (Cooperative Agreement No. AID-OAA-A-
215 14-00102). S.I. and S.F.M. are supported by NIH NIAID 4R01AI099210-04. ZIKV sequencing at
216 USAMRIID was supported by DARPA (PI: C. Kane). K.G.A. is a Pew Biomedical Scholar, and is
217 supported by NIH NCATS CTSA UL1TR001114, NIAID contract HHSN272201400048C, and The Ray
218 Thomas Foundation. The content of this publication does not necessarily reflect the views or policies of
219 the US Army, the Department of Health and Human Services, the CDC, or the Florida DOH.

220 **Author Contributions**

221 All contributions are listed in order of authorship. Designed the experiments: N.D.G., J.T.L., G.D.,
222 M.U.G.K., D.A.T.C., P.C.S., L.D.G., S.F.M., T.B., O.G.P., S.I., G.P., and K.G.A.; Collected samples:
223 A.L.T., S.W., D.M.M., A.B., L.M.P., D.P., P.N.L., M.R., V.K.B., D.I.W., M.R.C., E.W.K., K.N.H.,
224 A.C.C., R.J., M.C.P., C.V., D.S., L.D.G., S.F.M., and S.I.; Performed the sequencing: N.D.G., M.W.R.,
225 K.P., D.R., R.R.-S., G.O., and E.N.; Provided data, reagents, or protocols: N.D.G., J.T.L., G.D.,
226 M.U.G.K., K.G., M.R.W., R.R.-S., G.O., H.C.M., M.L.B., K.G.B., B.C., C.A.F., A.G.-Y., A.G., C.L.,
227 B.M., C.B.M., D.J.P., J.Q., S.F.S., C.T.-T., K.L.M., S.M.W., S.W., N.L.Y., J.Q., J.R.F., K.K., S.E.B.,
228 A.J.M., R.F.G., N.J.L., M.C.P., C.V., P.C.S., S.F.M., and S.I.; Analyzed the data: N.D.G., J.T.L., G.D.,
229 M.U.G.K., K.G., J.T., J.R.F., R.C.R., N.R.F., D.A.T.C., A.K., M.S.-L., T.B., S.F.M., O.G.P., S.I., and
230 K.G.A.; Edited manuscript: G.D., M.U.G.K., J.T., S.F.S., A.R., T.B., O.G.P., S.I., and G.P.; Wrote
231 manuscript: N.D.G., J.T.L., and K.G.A.; All authors read and approved the manuscript.

232 **Author Information**

233 The authors declare no competing financial interests. Correspondence and requests for materials should
234 be addressed to K.G.A (andersen@scripps.edu) or G.P. (gustavo.f.palacios.ctr@mail.mil).

235

280 **References**

- 281 1. Zika virus and complications. *World Health Organization* Available at:
282 <http://www.who.int/features/qa/zika/en/>. (Accessed: 1st November 2016)
- 283 2. Lazear, H. M. & Diamond, M. S. Zika Virus: New Clinical Syndromes and Its Emergence in the
284 Western Hemisphere. *J. Virol.* **90**, 4864–4875 (2016).
- 285 3. Likos, A. *et al.* Local Mosquito-Borne Transmission of Zika Virus - Miami-Dade and Broward
286 Counties, Florida, June-August 2016. *MMWR Morb. Mortal. Wkly. Rep.* **65**, 1032–1038 (2016).
- 287 4. Mosquito-Borne Disease Surveillance. *Florida Department of Health* Available at:
288 <http://www.floridahealth.gov/diseases-and-conditions/mosquito-borne-diseases/surveillance.html>.
289 (Accessed: 10th January 2017)
- 290 5. Hennessey, M., Fischer, M. & Staples, J. E. Zika Virus Spreads to New Areas — Region of the
291 Americas, May 2015–January 2016. *MMWR Morb. Mortal. Wkly. Rep.* **65**, 1–4 (2016).
- 292 6. Faria, N. R. *et al.* Zika virus in the Americas: Early epidemiological and genetic findings. *Science*
293 **352**, 345–349 (2016).
- 294 7. Faria, N. R., Quick, J., Morales, I., Theze, J. & de Jesus, J. G. Epidemic establishment and cryptic
295 transmission of Zika virus in Brazil and the Americas. *bioRxiv* (2017).
- 296 8. Metsky, H. C. *et al.* Genome sequencing reveals Zika virus diversity and spread in the Americas.
297 *bioRxiv* 109348 (2017). doi:10.1101/109348
- 298 9. Regional Zika Epidemiological Update (Americas). *Pan American Health Organization* (2016).
299 Available at:
300 http://www.paho.org/hq/index.php?option=com_content&view=article&id=11599&Itemid=41691&lang=en. (Accessed: 1st December 2016)
- 301
- 302 10. Weger-Lucarelli, J. *et al.* Vector Competence of American Mosquitoes for Three Strains of Zika
303 Virus. *PLoS Negl. Trop. Dis.* **10**, e0005101 (2016).
- 304 11. Guerbois, M. *et al.* Outbreak of Zika virus infection, Chiapas State, Mexico, 2015, and first
305 confirmed transmission by *Aedes aegypti* mosquitoes in the Americas. *J. Infect. Dis.* (2016).

- 306 12. Ferreira-de-Brito, A. *et al.* First detection of natural infection of *Aedes aegypti* with Zika virus in
307 Brazil and throughout South America. *Mem. Inst. Oswaldo Cruz* **0** (2016).
- 308 13. Chouin-Carneiro, T. *et al.* Differential Susceptibilities of *Aedes aegypti* and *Aedes albopictus* from
309 the Americas to Zika Virus. *PLoS Negl. Trop. Dis.* **10**, e0004543 (2016).
- 310 14. Kraemer, M. U. G. *et al.* The global distribution of the arbovirus vectors *Aedes aegypti* and *Ae.*
311 *albopictus*. *Elife* **4**, e08347 (2015).
- 312 15. Ferguson, N. M. *et al.* Countering the Zika epidemic in Latin America. *Science* **353**, 353–354
313 (2016).
- 314 16. Teets, F. D. *et al.* Origin of the dengue virus outbreak in Martin County, Florida, USA 2013. *Virol*
315 *Rep* **1-2**, 2–8 (2014).
- 316 17. Graham, A. S. *et al.* Mosquito-associated dengue virus, Key West, Florida, USA, 2010. *Emerg.*
317 *Infect. Dis.* **17**, 2074–2075 (2011).
- 318 18. Kendrick, K. *et al.* Notes from the field: transmission of chikungunya virus in the continental United
319 States—Florida, 2014. *MMWR Morb. Mortal. Wkly. Rep.* **63**, 1137 (2014).
- 320 19. Bouri, N. *et al.* Return of epidemic dengue in the United States: implications for the public health
321 practitioner. *Public Health Rep.* **127**, 259–266 (2012).
- 322 20. Ramos, M. M. *et al.* Epidemic Dengue and Dengue Hemorrhagic Fever at the Texas–Mexico Border:
323 Results of a Household-based Seroepidemiologic Survey, December 2005. *Am. J. Trop. Med. Hyg.*
324 **78**, 364–369 (2008).
- 325 21. Murray, K. O. *et al.* Identification of dengue fever cases in Houston, Texas, with evidence of
326 autochthonous transmission between 2003 and 2005. *Vector Borne Zoonotic Dis.* **13**, 835–845
327 (2013).
- 328 22. Monaghan, A. J. *et al.* On the Seasonal Occurrence and Abundance of the Zika Virus Vector
329 Mosquito *Aedes Aegypti* in the Contiguous United States. *PLoS Curr.* **8**, (2016).
- 330 23. Dzul-Manzanilla, F. *et al.* Evidence of vertical transmission and co-circulation of chikungunya and
331 dengue viruses in field populations of *Aedes aegypti* (L.) from Guerrero, Mexico. *Trans. R. Soc.*

- 332 *Trop. Med. Hyg.* **110**, 141–144 (2016).
- 333 24. Quick, J. *et al.* Multiplex PCR method for MinION and Illumina sequencing of Zika and other virus
334 genomes directly from clinical samples. *bioRxiv* 098913 (2017).
- 335 25. Drummond, A. J., Suchard, M. A., Xie, D. & Rambaut, A. Bayesian phylogenetics with BEAUti and
336 the BEAST 1.7. *Mol. Biol. Evol.* **29**, 1969–1973 (2012).
- 337 26. Robert, M. A. *et al.* Modeling Mosquito-Borne Disease Spread in U.S. Urbanized Areas: The Case
338 of Dengue in Miami. *PLoS One* **11**, e0161365 (2016).
- 339 27. McCarthy, M. First US case of Zika virus infection is identified in Texas. *BMJ* **352**, i212 (2016).
- 340 28. Nelson, B. *et al.* Travel Volume to the United States from Countries and U.S. Territories with Local
341 Zika Virus Transmission. *PLoS Curr.* **8**, (2016).
- 342 29. Dengue in Puerto Rico. *The Centers for Disease Control and Prevention* Available at:
343 <https://www.cdc.gov/dengue/about/inpuerto.html>. (Accessed: 17th March 2017)
- 344 30. Zika-Epidemiological Report. *Pan American Health Organization* Available at:
345 http://www.paho.org/hq/index.php?option=com_content&view=article&id=11603&Itemid=41696&lang=en. (Accessed: 1st December 2016)
- 346
- 347 31. Duffy, M. R. *et al.* Zika virus outbreak on Yap Island, Federated States of Micronesia. *N. Engl. J.*
348 *Med.* **360**, 2536–2543 (2009).
- 349 32. Dinh, L., Chowell, G., Mizumoto, K. & Nishiura, H. Estimating the subcritical transmissibility of the
350 Zika outbreak in the State of Florida, USA, 2016. *Theor. Biol. Med. Model.* **13**, 20 (2016).
- 351 33. Nunes, M. R. T. *et al.* Air travel is associated with intracontinental spread of dengue virus serotypes
352 1-3 in Brazil. *PLoS Negl. Trop. Dis.* **8**, e2769 (2014).
- 353 34. Basemaps. *ESRI* Available at: <http://www.esri.com/data/basemaps>. (Accessed: 1st October 2016)
- 354

236 **Figure Legends**

237 **Figure 1 | Zika virus outbreak in Florida.** (a) Weekly counts of confirmed travel-associated and
238 locally-acquired ZIKV cases in 2016. (b) Four counties reported locally-acquired ZIKV cases in 2016:
239 Miami-Dade (241), Broward (5), Palm Beach (8), Pinellas (1), and unknown origin (1). (c) The locations
240 of mosquito traps and collected *Ae. aegypti* mosquitoes found to contain ZIKV RNA (ZIKV+) in relation
241 to the transmission zones within Miami. (d) Temporal distribution of weekly ZIKV cases (left y-axis),
242 sequenced cases (bottom), and *Ae. aegypti* abundance per trap night (right y-axis) associated with the
243 three described transmission zones. ZIKV cases and sequences are plotted in relation to symptom onset
244 dates (n=18). Sequenced cases without onset dates or that occurred outside of the transmission zones are
245 not shown (n=10). Human cases and *Ae. aegypti* abundance per week were positively correlated
246 (Spearman $r = 0.61$, Extended Data Fig. 1b). The maps were generated using open source basemaps³⁴.

247
248 **Figure 2 | Multiple introductions of Zika virus into Florida.** (a) Maximum clade credibility (MCC)
249 tree of ZIKV genomes sequenced from outbreaks in the Pacific islands and the epidemic in the Americas.
250 Tips are colored based on collection location. The five tips outlined in blue but filled with a different
251 color indicate ZIKV cases in the United States associated with travel (fill color indicates the probable
252 location of infection). Clade posterior probabilities are indicated by white circles filled with black relative
253 to the level of support. The grey violin plot indicates the 95% highest posterior density (HPD) interval for
254 the tMRCA for the epidemic in the Americas (AM). Lineage F4 contains two identical ZIKV genomes
255 from the same patient. (b) A zoomed in version of the whole MCC tree showing the collection locations
256 of Miami-Dade sequences and whether they were sequenced from mosquitoes (numbers correspond to
257 trap locations in Fig. 1c). 95% HPD intervals are shown for the tMRCAs (c) The probability of ZIKV
258 persistence after introduction for different R_0 . Persistence is measured as the number of days from initial
259 introduction of viral lineages until their extinction. Vertical dashed lines show the inferred mean
260 persistence time for lineages F1, F2 and B based on their tMRCA. (d) Total number of introductions
261 (mean with 95% CI) that contributed to the outbreak of 241 local cases in Miami-Dade County for
262 different R_0 .

263
264 **Figure 3 | Frequent opportunities for Zika virus introductions into Miami from the Caribbean.** (a)
265 Reported ZIKV cases per country/territory from January to June, 2016 normalized by total population. (b)
266 The number of estimated travelers entering Miami during January to June, 2016 by method of travel. (c)
267 The number of travelers and the reported ZIKV incidence rate for the country/territory of origin were
268 used to estimate the proportion of infected travelers coming from each region with ZIKV in the Americas.
269 (d) The observed number of weekly travel-associated ZIKV cases in Florida were plotted with the
270 expected number of ZIKV-infected travelers (as estimated in panel c) coming from all of the Americas
271 (grey line) and the regional contributions (colored areas). (e) The countries visited by the 1,016 travel-
272 associated ZIKV cases diagnosed in Florida.

273
274 **Figure 4 | Southern Florida has a high potential for *Aedes aegypti*-borne virus outbreaks.** The
275 estimated number of travelers per month (circles) entering Florida cities via flights and cruise ships were
276 plotted with estimated relative *Ae. aegypti* abundance. Only cities receiving >10,000 passengers per
277 month are shown. Relative *Ae. aegypti* abundance for every month is shown in Extended Data Fig. 1d.

278
279

Fig 1.

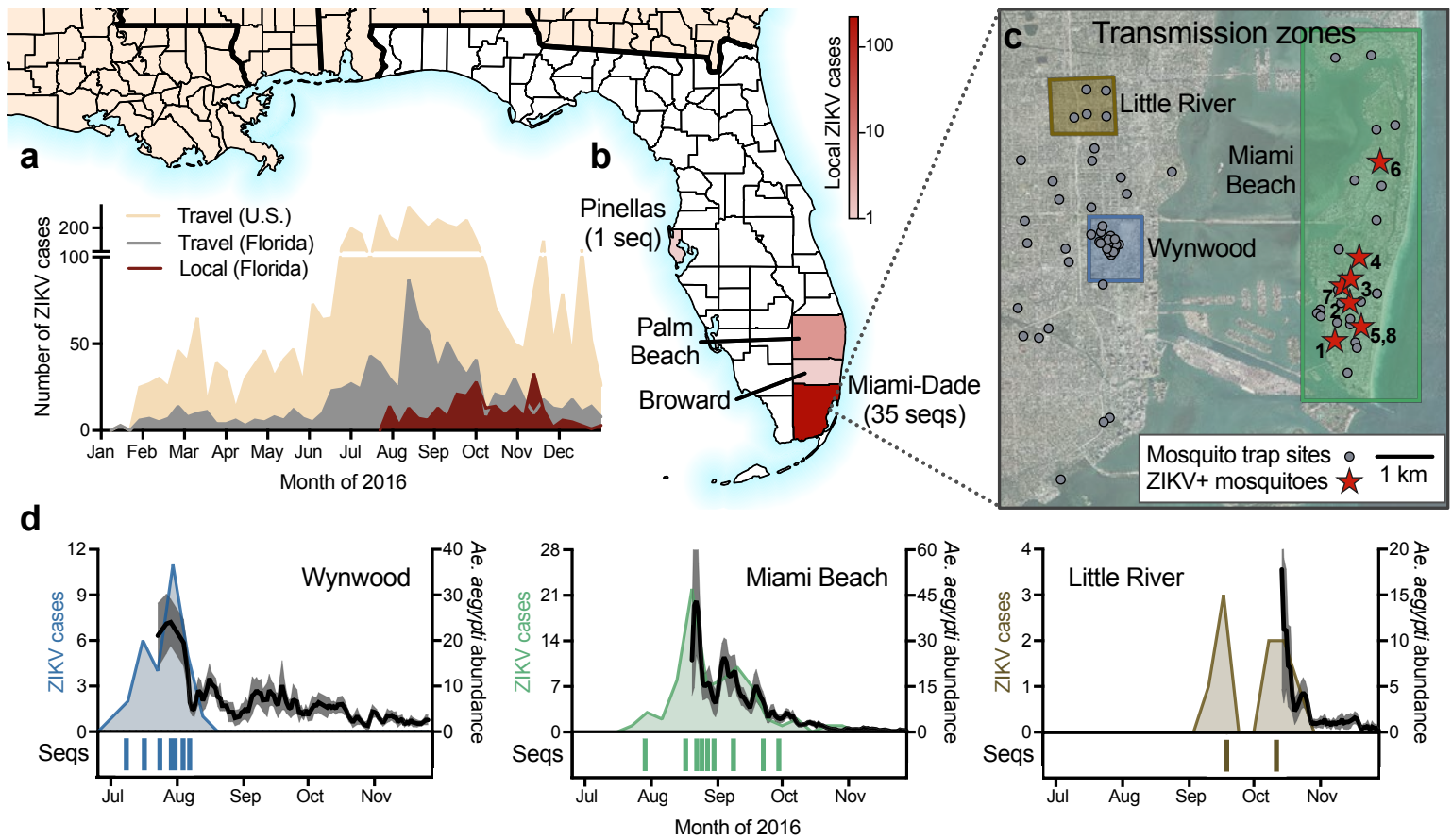


Fig 2.

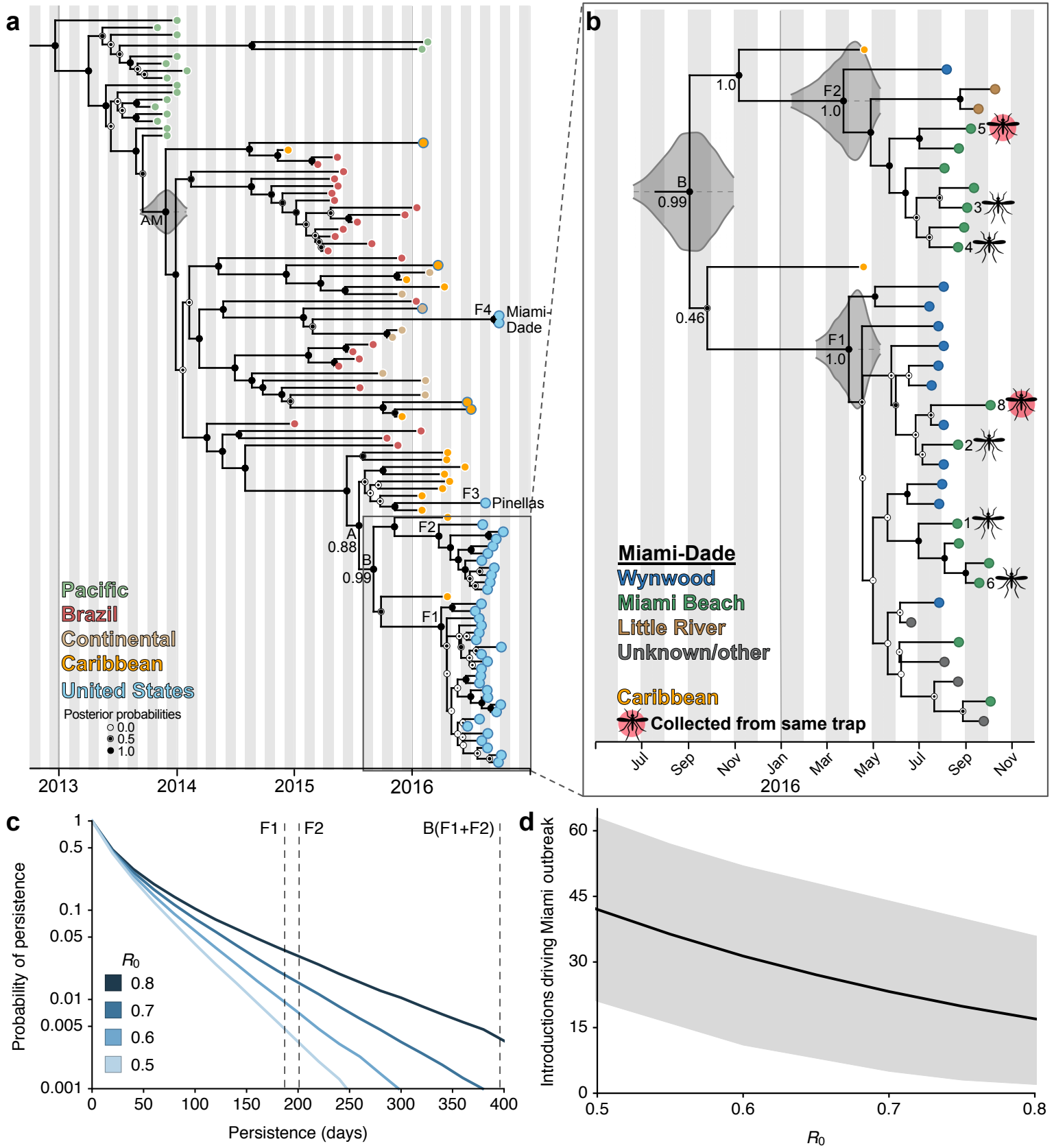


Fig 3.

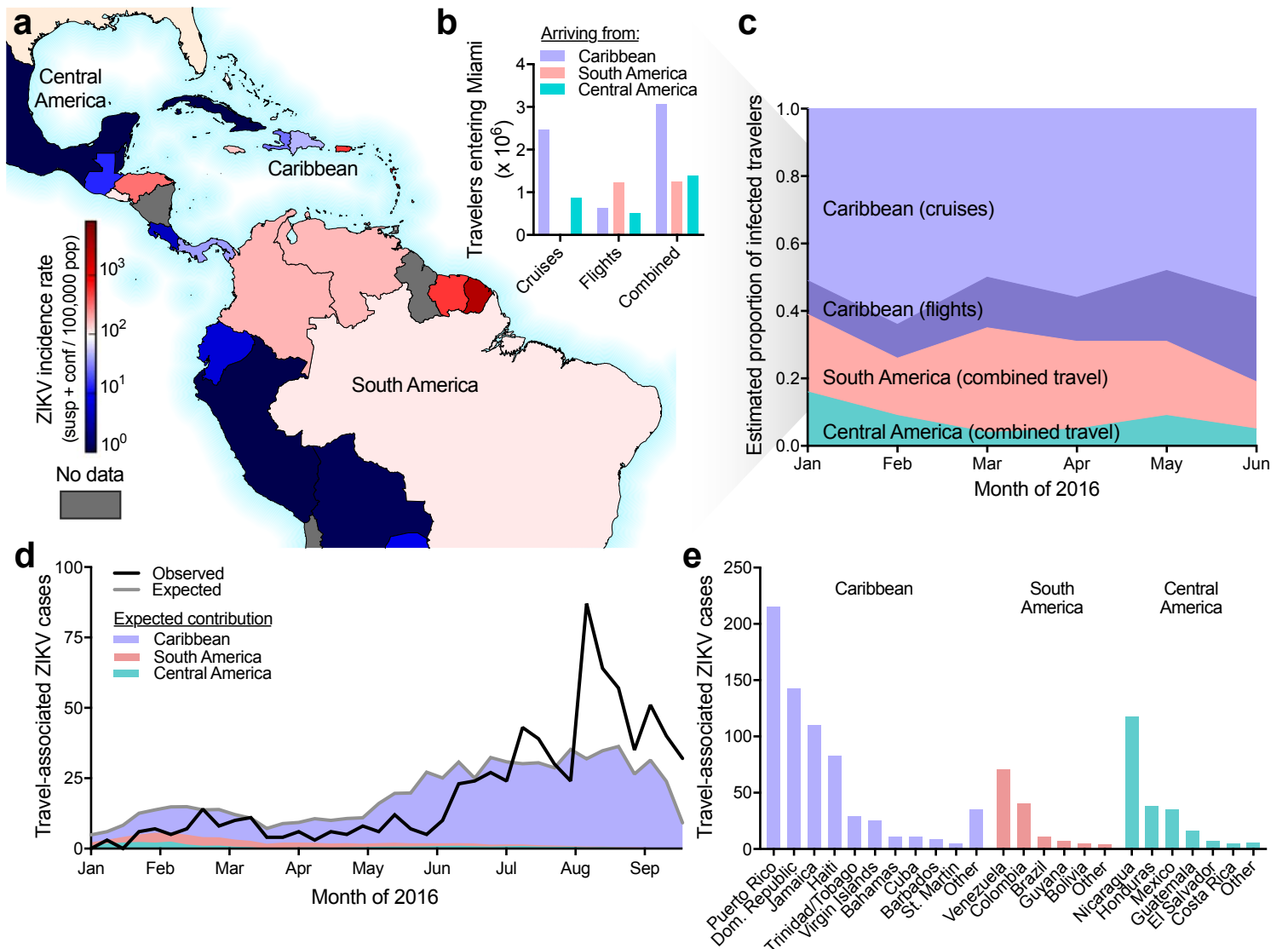
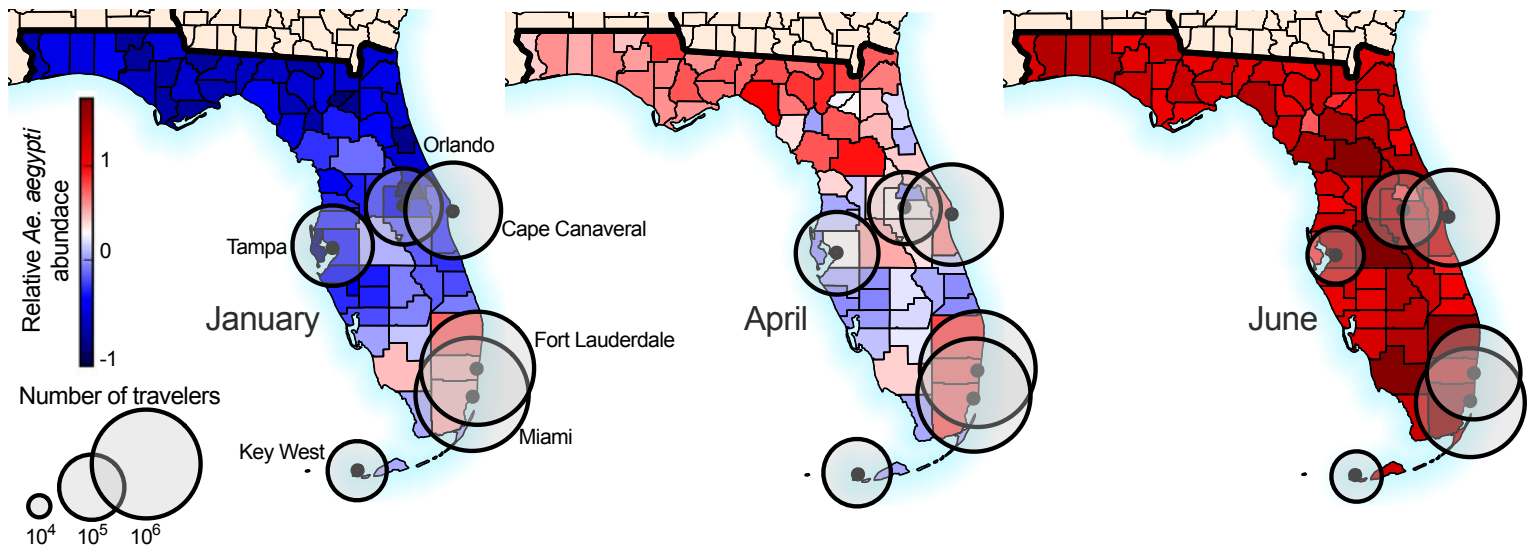


Fig 4.



355 **Methods**

356 **Ethical statement**

357 This work was evaluated and approved by relevant Institutional Review Boards (IRB)/Ethics Review
358 Committees at The Scripps Research Institute (TSRI) and the US Army Medical Research Institute of
359 Infectious Diseases (USAMRIID) Office of Human Use and Ethics. This work was conducted as part of
360 the public health response in Florida and samples were collected under a waiver of consent granted by the
361 Florida DOH Human Research Protection Program. The work received a non-human subjects research
362 designation (category 4 exemption) by the Florida DOH since this research was performed with leftover
363 clinical diagnostic samples involving no more than minimal risk. All samples were deidentified prior to
364 receipt by the study investigators.

365 **Florida Zika virus case data**

366 Weekly reports of international travel-associated and locally-acquired ZIKV infections diagnosed in
367 Florida were obtained from the Florida DOH mosquito-borne disease surveillance system⁴. Dates of
368 symptom onset from the Miami transmission zones (Wynwood, Miami Beach, and Little River)
369 determined by the Florida DOH investigation process were obtained from the ZIKV resource website³⁵
370 and daily updates³⁶. International travel-associated ZIKV case counts in the United States (outside of
371 Florida) were obtained from the CDC³⁷. The local and travel-associated ZIKV case numbers for Florida
372 were obtained from the Florida DOH. The one local ZIKV infection diagnosed in Duval County was
373 believed to have originated elsewhere in Florida. Therefore, this case is listed as “unknown origin” in Fig.
374 1b. In Fig. 3e, only the countries visited by 5 or more times by ZIKV-infected travelers diagnosed in
375 Florida are shown. Countries with 5 or fewer visits were aggregated into an “other” category by region
376 (*i.e.*, Caribbean, South America, or Central America).

377 **Clinical sample collection and RNA extraction**

378 Clinical samples from locally-acquired ZIKV infections were collected from June 22 to October 11, 2016.
379 The Florida DOH identified persons with compatible illness and clinical samples were shipped to the
380 Bureau of Public Health Laboratories for confirmation by qRT-PCR and antibody tests following interim
381 guidelines^{3,38-40}. Clinical specimens (whole blood, serum, saliva, or urine) submitted for analysis were
382 refrigerated or frozen at $\leq -70^{\circ}\text{C}$ until RNA was extracted. RNA was extracted using the RNAeasy kit
383 (QIAGEN), MagMAX for Microarrays Total RNA Isolation Kit (Ambion), or MagNA Pure LC 2.0 or 96
384 Systems (Roche Diagnostics). Purified RNA was eluted into 50-100 μL using the supplied elution
385 buffers, immediately frozen at $\leq -70^{\circ}\text{C}$, and transported on dry ice. The Florida DOH also provided
386 investigation data for these samples, including symptom onset dates and, when available, assignments to
387 the zone where infection likely occurred (Supplementary Table 1).

388 **Mosquito collection, RNA extraction, and entomological data analysis**

389 24,351 *Ae. aegypti* and *Ae. albopictus* mosquitoes (sorted into 2,596 pools) were collected throughout
390 Miami-Dade County during June to November, 2016 using BG-Sentinel mosquito traps (Biogents AG).
391 Up to 50 mosquitoes of the same species and sex were pooled per trap. The pooled mosquitoes were
392 stored in RNAlater (Invitrogen), RNA was extracted using either the RNAeasy kit (QIAGEN) or
393 MagMAX for Microarrays Total RNA Isolation Kit (Ambion), and ZIKV RNA was detected by qRT-
394 PCR targeting the envelope protein coding region⁴⁰ or the Trioplex qRT-PCR kit⁴¹. ZIKV infection rates
395 were calculated per 1,000 female *Ae. aegypti* mosquitoes using the bias-corrected maximum likelihood
396 estimate (MLE)⁴². Days of insecticide usage by the Miami-Dade Mosquito Control were inferred from the
397 zone-specific ZIKV activities timelines published by the Florida DOH³⁵.

398 **Relative monthly *Ae. aegypti* abundance**

399 For the purpose of this study we used *Ae. aegypti* suitability maps from Kraemer *et al.*¹⁴ and derived
400 monthly estimates based on the statistical relationships between mosquito presence and environmental
401 correlates⁴³. Following Hwang *et al.*⁴⁴ we used a simple mathematical formula to transform the
402 probability of detection maps into mosquito abundance maps. In order to do so, we assumed $P(Y=1)$
403 where Y is a binary variable (presence/absence). Using a Poisson distribution $X()$ to govern the
404 abundance of mosquitoes, the probability of not observing any mosquitoes can be related to the
405 probability of absence as: $P(X=0)=P(Y=0)$. We used the following transformation to generate abundance
406 (λ) estimates per county in Florida:

$$e^{-\lambda} = P(Y = 0)$$

$$\lambda = -\log(P(Y = 0))$$

$$\lambda = -\log(1 - P(Y = 1))$$

407 We did not consider *Ae. albopictus* abundance in this study because 99.8% of mosquitoes collected in
408 Miami-Dade County were *Ae. aegypti*. Relative *Ae. aegypti* abundance in major U.S. cities presented in
409 Extended Data Fig. 8 was estimated as previously described²².

410 **Zika virus quantification**

411 ZIKV genome equivalents (GE) were quantified by qRT-PCR. At TSRI, ZIKV qRT-PCR was performed
412 as follows: ZIKV RNA standards were transcribed from the ZIKV NS5 region (8651-9498 nt) using the
413 T7 forward primer (5' - TAA TAC GAC TCA CTA TAG GGA GA TCA GGC TCC TGT CAA AAC
414 CC - 3'), reverse primer (5' - AGT GAC AAC TTG TCC GCT CC - 3'), and the T7 Megascript kit
415 (Ambion). For qRT-PCR, primers and a probe targeting the NS5 region (9014-9123 nt) were designed
416 using the ZIKV isolate PRVABC59 (GenBank: KU501215): forward primer (5' - AGT GCC AGA GCT
417 GTG TGT AC - 3'), reverse primer (5' - TCT AGC CCC TAG CCA CAT GT - 3'), and FAM-fluorescent
418 probe (5' - GGC AGC CGC GCC ATC TGG T - 3'). The qRT-PCR assays were performed in 25 μ l
419 reactions using the iScript One-step RT-PCR Kit for probes (Bio-Rad Laboratories Inc.) and 2 μ l of
420 sample RNA. Amplification was performed at 50°C for 20 min, 95°C for 3 min, and 40 cycles of 95°C
421 for 10 s and 57°C for 10 s. Fluorescence was read at the end of the 57°C annealing-extension step. 10-fold
422 dilutions of the ZIKV RNA transcripts (2 μ l/reaction) were used to create a standard curve for
423 quantification of ZIKV GE/ μ l of RNA. The lower limits of quantification are 4 GE/ μ l RNA, or at a cycle
424 threshold of ~36.

425 ZIKV GE were quantified at USAMRIID using the University of Bonn ZIKV envelope protein (Bonn E)
426 qRT-PCR assay⁴⁵. RNA standards were transcribed using an amplicon generated from a ZIKV plasmid
427 containing T7 promoter at the start of the 5' untranslated region (UTR). The plasmid was designed using
428 the ZIKV isolate BeH819015 (GenBank: KU365778.1) and the amplicon included nts 1-4348, which
429 covers the 5' UTR, C, prM, M, E, NS1, and NS2 regions. The qRT-PCR assays were performed in 25 μ l
430 reactions using the SuperScript III platinum One-step qRT-PCR Kit (ThermoFisher) and 2 μ l of sample
431 RNA was used. Amplification was performed following conditions as previously described⁴⁵. 10-fold
432 dilutions of the ZIKV RNA transcripts (5 μ l/reaction) were used to create a standard curve for
433 quantification of ZIKV GE/ μ l of RNA.

434 **Amplicon-based Zika virus sequencing**

435 ZIKV sequencing at TSRI was performed using an amplicon-based approach using the ZikaAsian V1
436 scheme, as described²⁴. This approach is similar to “RNA jackhammering” to sequence low-quality viral
437 samples developed by Worobey *et al.*⁴⁶. Briefly, cDNA was reverse transcribed from 5 μ l of RNA using
438 SuperScript IV (Invitrogen). ZIKV cDNA (2.5 μ l/reaction) was amplified in 35 \times 400 bp fragments from
439 two multiplexed PCR reactions using Q5 DNA High-fidelity Polymerase (New England Biolabs). The

440 amplified ZIKV cDNA fragments (50 ng) were prepared for sequencing using the Kapa Hyper prep kit
441 (Kapa Biosystems) and SureSelect XT2 indexes (Agilent). Agencourt AMPure XP beads (Beckman
442 Coulter) were used for all purification steps. Paired-end 251 nt reads were generated on the MiSeq using
443 the V2 500 cycle or V3 600 cycle kits (Illumina).

444 Trimmomatic was used to remove primer sequences (first 22 nt from the 5' end of the reads, which is the
445 maximum length of the primers used for the multiplexed PCR) and bases at both ends with Phred quality
446 score < 20⁴⁷. The reads were then aligned to the complete genome of a ZIKV isolate from the Dominican
447 Republic, 2016 (GenBank: KU853012) using Novoalign v3.04.04 (www.novocraft.com). Samtools was
448 used to sort the aligned BAM files and to generate alignment statistics⁴⁸. Snakemake was used as the
449 workflow management system⁴⁹. The code and reference indexes for the pipeline can be found at
450 <https://github.com/andersen-lab/zika-pipeline>. ZIKV-aligned reads were visually inspected using
451 Geneious v9.1.5⁵⁰ before generating consensus sequences. A minimum of 3× read-depth coverage, in
452 support of the consensus, was required to make a base call.

453 **Enrichment-based Zika virus sequencing**

454 ZIKV sequencing at USAMRIID was performed using a targeted enrichment approach. Sequencing
455 libraries were prepared using the TruSeq RNA Access Library Prep kit (Illumina) with custom ZIKV
456 probes. The set included 866 unique probes each of which was 80 nt in length (Supplementary Table 2a).
457 The probes were designed to cover the entire ZIKV genome and to encompass the genetic diversity
458 present on GenBank on January 14, 2016. In total, 26 ZIKV sequences were used during probe design
459 (Supplementary Table 2b). Extracted RNA was fragmented at 94 °C for 0-60 s and each sample was
460 enriched separately using a quarter of the reagents specified in the manufacturer's protocol. Samples were
461 barcoded, pooled and sequenced using the MiSeq Reagent kit v3 (Illumina) on an Illumina MiSeq with a
462 minimum of 2 × 151 bp reads. Dual indexing, with no overlapping indices, was used.

463 The random hexamer associated with read one and the Illumina adaptors were removed from the
464 sequencing reads using Cutadapt v1.9.dev1⁵¹, and low-quality reads/bases were filtered using Prinseq-lite
465 v0.20.3⁵². Reads were aligned to a reference genome (GenBank: KX197192.1) using Bowtie2 v2.0.6⁵³,
466 duplicates were removed with Picard (<http://broadinstitute.github.io/picard>), and a new consensus was
467 generated using a combination of Samtools v0.1.18⁴⁸ and custom scripts
468 (https://github.com/jtladner/Scripts/blob/master/reference-based_assembly/consensus_fasta.py). Only
469 bases with Phred quality score ≥ 20 were utilized in consensus calling, and a minimum of 3× read-depth
470 coverage, in support of the consensus, was required to make a call; positions lacking this depth of
471 coverage were treated as missing (*i.e.* called as ‘N’).

472 **Validation and comparison of sequencing methods**

473 The consensus ZIKV sequences from FL01M and FL03M generated by sequencing 35 × 400 bp
474 amplicons on the MiSeq were validated using the following approaches: 1) sequencing the 35 × 400 bp
475 amplicons on the Ion S5 platform (ThermoFisher), 2) sequencing amplicons generated using an Ion
476 AmpliSeq® (ThermoFisher) panel customly targeted towards ZIKV on the Ion S5 platform, and 3)
477 sequencing 5 × 2,150-2,400 bp ZIKV amplicons on the MiSeq. For Ion library preparation, cDNA was
478 synthesized using the SuperScript VILO kit (ThermoFisher). ThermoFisher designed 875 custom ZIKV
479 primers to produce 75 amplicons of ~200 bp in two PCR reactions for use with their Ion AmpliSeq
480 Library Kit 2.0. The reagent FuPa was used to digest the modified primer sequences after amplification.
481 The DNA templates were loaded onto Ion 520 chips using the Ion Chef and sequenced on the Ion S5 with
482 the 200 bp output (ThermoFisher). The 35 × 400 bp amplicons generated for the MiSeq as described
483 above were introduced into the Ion workflow using the Ion AmpliSeq Library Kit 2.0, but without
484 fragmentation. Primers to amplify 2,150-2,400 bp ZIKV fragments (Supplementary Table 2c) were kindly
485 provided by Shelby O'Connor, Dawn Dudley, Dave O'Connor, and Dane Gellerup (AIDS Vaccine
486 Research Laboratory, University of Wisconsin, Madison). Each fragment was amplified individually by

487 PCR using the cDNA generated above, Q5 DNA High-fidelity Polymerase, and the following
488 thermocycle conditions: 55 °C for 30 m, 94 °C for 2 m, 35 cycles of 94 °C for 15 s, 56 °C for 30 s, and 68
489 °C for 3.5 m, 68 °C for 10 m, and held at 4 °C until use. Each PCR product was purified using Agencourt
490 AMPure XP beads, sheared to 300 to 400 nt fragments using the Covaris S2 sonicator, indexed and
491 prepared for sequencing as described above, and sequenced using the MiSeq V2 500 cycle kit (paired-end
492 251 nt reads). Compared to the consensus sequences generated using 35 × 400 bp amplicons on the
493 MiSeq, there were no consensus-level mismatches in the coding sequence using any of the other three
494 approaches (Extended Data Table 2). There were, however, some mismatches in the 5' and 3' UTRs
495 (where the genomic RNA is heavily structured), likely a result of PCR bias and decreased coverage depth.

496 At least 95% of the ZIKV genome was covered from samples with as low as 4 and 9 GE/μl RNA from the
497 amplicon and enrichment approaches, respectively. These results are similar to our previously determined
498 clinical range of 10-16 ZIKV GE/μl RNA to achieve at least 95% genome coverage using our amplicon-
499 based approach²⁴. On average, the amplicon-based sequencing approach covered 97% of the ZIKV
500 genome ($\geq 3\times$ read-depth) and the targeted enrichment approach covered 82% of the ZIKV genome from
501 clinical samples (Supplementary Table 2d).

502 **Phylogenetic analyses**

503 All published and available complete ZIKV genomes of the Asian genotype from the Pacific and the
504 Americas were retrieved from GenBank public database as of December 2016. Public sequences (n=65)
505 were codon-aligned together with ZIKV genomes generated in this study (n=39) using MAFFT⁵⁴ and
506 inspected manually. The multiple alignment contained 104 ZIKV sequences collected between 2013 and
507 2016, from the Pacific (American Samoa, French Polynesia, and Tonga), Brazil, other South and Central
508 Americas (Guatemala, Mexico, Suriname, and Venezuela), the Caribbean (Dominican Republic,
509 Guadeloupe, Haiti, Martinique, and Puerto Rico), and the United States (Supplementary File 1).

510 In order to determine the temporal signal of the sequence dataset, a maximum likelihood (ML) phylogeny
511 was first reconstructed with PhyML⁵⁵ using the general time-reversible (GTR) nucleotide substitution
512 model and gamma distributed rates amongst sites⁵⁶ (Supplementary File 1), which was identified as the
513 best fitting model for ML inference by jModelTest⁵⁷. Then, a correlation between root-to-tip genetic
514 divergence and date of sampling was conducted in TempEst⁵⁸.

515 Bayesian phylogenetic analyses were performed using BEAST v.1.8.4²⁵ to infer time-structured
516 phylogenies. We used an SDR06 nucleotide substitution model⁵⁹ with a non-informative continuous time
517 Markov chain reference prior (CTMC)⁶⁰ on the molecular clock rate. Replicate analyses using multiple
518 combinations of molecular clock and coalescent models were explored to select the best fitting model by
519 marginal likelihood comparison using path-sampling and stepping-stone estimation approaches⁶¹⁻⁶³
520 (Extended Data Table 1b). The best fit model was a relaxed molecular clock along with a Bayesian
521 Skyline model⁶⁴. All the Bayesian analyses were run for 30 million Markov chain Monte Carlo steps,
522 sampling parameters and trees every 3000 generations (BEAST XML file and MCC tree available in
523 Supplementary File 1). Support values for all nodes are embedded in the phylogenetic tree files
524 (Supplementary File 1). Tree visualizations were generated with baltic (github.com/blab/baltic).

525 The travel-associated ZIKV genomes add to the Caribbean dataset, but do not directly influence our
526 conclusions about the source of ZIKV introductions into Florida.

527 **Expected number and distribution of local cases from Zika virus importations**

528 We used branching process theory^{65,66} to generate the offspring distribution (subsequent local cases) that
529 is expected from a single introduction. The offspring distribution L is modelled with a negative binomial
530 distribution with mean R_0 and over-dispersion parameter k . The total number of cases j that is caused by a
531 single importation (including the index case) after an infinite time⁶⁷ has the following form:

$$L = \frac{\Gamma(kj + j - 1)}{\Gamma(kj) \Gamma(j + 1)} \frac{\left(\frac{R_0}{k}\right)^{j-1}}{\left(1 + \frac{R_0}{k}\right)^{kj+j-1}}$$

532 The parameter k represents the variation in the number of secondary cases generated by each case of
 533 ZIKV⁶⁵. In the case of vector borne diseases, local heterogeneity is high due to a variety of factors such as
 534 mosquito population abundance, human to mosquito interaction, and control interventions^{68–73}. Here, we
 535 assumed high heterogeneity ($k=0.1$) following previous estimates for vector borne diseases⁶⁶. This
 536 distribution L is plotted in Extended Data Fig. 4a. For the following, we took a forward simulation
 537 approach, drawing random samples from this distribution. All estimates were based on 100,000 random
 538 simulations.

539 We used this formula to estimate the probability of observing 241 local cases in Miami-Dade County
 540 alongside 320 travel-associated cases. We approached this by sampling 320 introduction events from L
 541 and calculating the total number of local cases in the resulting outbreak (Extended Data Fig. 4b). We also
 542 calculated the likelihood of observing 241 local cases in the total outbreak (Extended Data Fig. 4c),
 543 finding that the MLE of R_0 lies between 0.35 and 0.55. As a sensitivity analysis, we additionally modelled
 544 introductions with the assumption that only 50% of travelers were infectious at time of arrival into
 545 Miami-Dade County, resulting in an MLE of R_0 of 0.45–0.8.

546 We further used this formula to address the probability of observing 3 distinct genetic clusters (F1, F2 and
 547 F3) representing 3 introduction events in a sample of 27 ZIKV genomes from Miami-Dade County. We
 548 approached this by sampling introduction events until we accumulated 241 local cases according to L ,
 549 arriving at N introduction events with case counts (j_1, j_2, \dots, j_N) . We then sampled 27 cases *without*
 550 *replacement* from (j_1, j_2, \dots, j_N) following a hypergeometric distribution and recorded the number of
 551 distinct clusters drawn in the sample. We found that higher values of R_0 resulted in fewer distinct clusters
 552 within the sample of 27 genomes (Extended Data Fig. 4d). We additionally calculated the likelihood of
 553 sampling 3 distinct genetic clusters in 27 genomes (Extended Data Fig. 4e), finding an MLE estimate of
 554 R_0 of 0.7–0.9. Additionally, as a sensitivity analysis we modelled a preferential sampling process in which
 555 larger clusters are more likely to be drawn from than smaller clusters. Here, we used a parameter α that
 556 enriches the hypergeometric distribution following $(j_1^\alpha, j_2^\alpha, \dots, j_N^\alpha)$. In this case, we found an MLE
 557 estimate of R_0 of 0.5–0.9.

558 Using the overlap of estimates of R_0 from local case counts (0.35–0.8) and genetic clusters (0.5–0.9), we
 559 arrived at a 95% uncertainty range of R_0 of 0.5–0.8. As an additional sensitivity analysis, we incorporated
 560 under-reporting in which either 50% of travel-associated cases and 25% of local cases are reported or in
 561 which 10% of travel-associated cases and 5% of local cases are reported. We find differential reporting of
 562 travel and local cases results in increased mean R_0 estimates when comparing counts of travel-associated
 563 to local cases (Extended Data Figure 4f-g). Additionally, we find that under-reporting increases estimates
 564 of R_0 from the sampling analysis (Extended Data Figure 4h-i). Thus, moderate under-reporting is
 565 consistent with R_0 estimates of ~ 0.8 .

566 We additionally perform birth-death stochastic simulations assuming a serial interval with mean 20
 567 days¹⁵. We record the number of stochastic simulations still persisting after a particular number of days
 568 for different values of R_0 (Fig. 2c).

569 **Zika virus incidence rates**

570 Weekly suspected and confirmed ZIKV case counts from countries and territories within the Americas
 571 with local transmission (January 1 to September 18, 2016) were obtained from the Pan American Health
 572 Organization (PAHO)³⁰. In most cases, the weekly case numbers per country were only reported in bar
 573 graphs. We contacted PAHO multiple times with the hope of gaining access to the raw data included in

574 the bar graphs, but our requests were unfortunately denied. Therefore we used WebPlotDigitizer v3.10
575 (<http://arohatgi.info/WebPlotDigitizer>) to estimate the numbers. We compared the actual ZIKV case
576 numbers reported in Ecuador⁷⁴ (only country with available raw data and reported cases > 10 per week) to
577 our estimates from the PAHO bar graphs and found that the WebPlotDigitizer was ~99% accurate
578 (Extended Data Fig. 5a-b).

579 Country and territory total population sizes to calculate weekly and monthly ZIKV incidence rates were
580 also obtained from PAHO⁷⁵. Incidence rates calculated from countries and territories in the Americas
581 during January to June, 2016 (based on the earliest introduction time estimates until the first known cases)
582 were used as an estimate for infection likelihood to investigate sources of ZIKV introductions.

583 **Airline and cruise ship traffic**

584 To investigate whether the transmission of ZIKV in Florida coincides with travel patterns from ZIKV
585 endemic regions, we obtained the number of passengers arriving at airports in Florida via commercial air
586 travel. We collated flight data from countries and territories in the Americas with local ZIKV
587 transmission between January and June, 2016 (based on the earliest introduction time estimates until the
588 first known cases, Supplementary Table 1b), arriving at all commercial airports in Florida. The data were
589 obtained from the International Air Transportation Association, which collects data on an estimated 90%
590 of all passenger trips worldwide. Nelson *et al.*²⁸ previously reported flight data from 33 countries with
591 ZIKV transmission entering major United States airports during October 2014 through September 2015,
592 which we used to assess the potential for ZIKV introductions outside of Florida.

593 Schedules for cruise ships visiting Miami, Port Canaveral, Port Everglades, Fort Lauderdale, Key West,
594 Jacksonville (all in Florida), Houston, Galveston (both in Texas), Charleston (South Carolina) and New
595 Orleans (Louisiana) ports in the year 2016 were collated from www.cruisett.com and confirmed by cross-
596 referencing ship logs reported by Port of Miami and reported ship schedules from
597 www.miamidade.gov/portmiami/. Scheduled cruise ship capacities were extracted from
598 www.cruisemapper.com. Every country/territory with ZIKV transmission visited by a cruise ship 10 days
599 (the approximate mean time to ZIKV clearance in human blood [*i.e.*, the infectious period])⁷⁶ prior to
600 arrival was counted as contributing the ship's capacity worth of passengers to Miami to the month of
601 arrival (Supplementary Table 1b). While the air traffic was based on the reported number of travelers, we
602 estimated the sea traffic by ship capacity. Lee and Ramdeen⁷⁷ reported that the average occupancy of
603 cruise ships traveling to the Caribbean Islands exceeded 100% in 2011, and according to the Florida-
604 Caribbean Cruise Association⁷⁸, it remained >100% in 2015. Occupancy data for 2016 was not available
605 at the time of publication, but we assumed that it was also near 100%.

606 **Expected number of travelers infected with Zika virus**

607 We estimated the expected number of travelers entering Miami who were infected with ZIKV (λ) by
608 using the total travel capacity (C) and the likelihood of ZIKV infection (infections (I) per person (N))
609 from each country/territory (i):

$$\lambda = \sum_i C_i \frac{I_i}{N_i}$$

610 We summed the number of expected infected travelers from each country/territory with ZIKV
611 transmission by region and travel method (flights or cruises). The number of ZIKV cases reported by each
612 country are likely under-estimates in part because the majority of ZIKV infections are asymptomatic^{2,31}.
613 We normalized some of the potential reporting variances between countries by reporting the data as the
614 relative proportion of infected travelers (Fig. 3c, Extended Data Fig. 7a) and as the absolute number of
615 infected travelers (Fig. 3d, Extended Data Fig. 7b, Supplementary Table 1b) from each region. We also
616 accounted for potential reporting biases with incidence rates by using ZIKV attack rates (*i.e.*, proportion

617 infected before epidemic burnout) to estimate peak transmission intensity. Attack rates were calculated
618 using a susceptible–infected–recovered (SIR) transmission model derived from seroprevalence studies
619 and environmental factors as described⁷⁹. Using attack rates as an estimate of infection likelihood, we
620 predict that ~60% of the infected travelers entering Miami came from the Caribbean (Extended Data 7b),
621 which is in agreement with our methods using incidence rates of ~60-70% (Fig. 3c). A list of countries
622 and territories used in these analyses can be found in Supplementary Table 1b.

623 **Maps**

624 The maps presented in our figures were generated using Matplotlib⁸⁰ and ESRI basemaps
625 (www.esri.com/data/basemaps). The software and basemaps are open source and “freely available to
626 anyone”.

627 **Data availability**

628 All ZIKV sequencing data is available under the NCBI BioProjects PRJNA342539 and PRJNA356429.
629 Individual sample GenBank access numbers are listed in Supplementary Table 1a. All other data is
630 available in the Extended Data, Supplemental Information, or upon request.

631

632

633

755 **Extended References**

- 756 35. Zika virus. *Florida Department of Health* Available at: [http://www.floridahealth.gov/diseases-and-](http://www.floridahealth.gov/diseases-and-conditions/zika-virus/index.html?utm_source=flhealthIndex)
757 [conditions/zika-virus/index.html?utm_source=flhealthIndex](http://www.floridahealth.gov/diseases-and-conditions/zika-virus/index.html?utm_source=flhealthIndex). (Accessed: 10th January 2017)
- 758 36. Daily Zika update. *Florida Department of Health* Available at:
759 <http://www.floridahealth.gov/newsroom/all-articles.html>. (Accessed: 10th January 2017)
- 760 37. Zika virus case counts in the US. *The Centers for Disease Control and Prevention* (2016). Available
761 at: <http://www.cdc.gov/zika/geo/united-states.html>. (Accessed: 10th January 2017)
- 762 38. Rabe, I. B. *et al.* Interim Guidance for Interpretation of Zika Virus Antibody Test Results. *MMWR*
763 *Morb. Mortal. Wkly. Rep.* **65**, 543–546 (2016).
- 764 39. Waggoner, J. J. & Pinsky, B. A. Zika Virus: Diagnostics for an Emerging Pandemic Threat. *J. Clin.*
765 *Microbiol.* **54**, 860–867 (2016).
- 766 40. Lanciotti, R. S. *et al.* Genetic and serologic properties of Zika virus associated with an epidemic,
767 Yap State, Micronesia, 2007. *Emerg. Infect. Dis.* **14**, 1232–1239 (2008).
- 768 41. Interim Guidance for Zika Virus Testing of Urine - United States, 2016. *MMWR Morb. Mortal.*
769 *Wkly. Rep.* **65**, 474 (2016).
- 770 42. Biggerstaff, B. PooledInfRate, version 4.0. *An Excel Add-In to Compute Infection Rates from Pooled*
771 *Data. Centers for Disease Control, Fort Collins, CO* (2009).
- 772 43. Bogoch, I. I. *et al.* Potential for Zika virus introduction and transmission in resource-limited
773 countries in Africa and the Asia-Pacific region: a modelling study. *Lancet Infect. Dis.* (2016).
774 doi:10.1016/S1473-3099(16)30270-5
- 775 44. Hwang, W.-H. & He, F. Estimating abundance from presence/absence maps. *Methods Ecol. Evol.* **2**,
776 550–559 (2011).
- 777 45. Corman, V. M. *et al.* Clinical comparison, standardization and optimization of Zika virus molecular
778 detection. *Bull. World Health Organ.* (2016).
- 779 46. Worobey, M. *et al.* 1970s and ‘Patient 0’ HIV-1 genomes illuminate early HIV/AIDS history in
780 North America. *Nature* (2016). doi:10.1038/nature19827

- 781 47. Bolger, A. M., Lohse, M. & Usadel, B. Trimmomatic: a flexible trimmer for Illumina sequence data.
782 *Bioinformatics* **30**, 2114–2120 (2014).
- 783 48. Li, H. *et al.* The Sequence Alignment/Map format and SAMtools. *Bioinformatics* **25**, 2078–2079
784 (2009).
- 785 49. Köster, J. & Rahmann, S. Building and documenting workflows with python-based snakemake. in
786 *OASISs-OpenAccess Series in Informatics* **26**, (Schloss Dagstuhl-Leibniz-Zentrum fuer Informatik,
787 2012).
- 788 50. Kears, M. *et al.* Geneious Basic: an integrated and extendable desktop software platform for the
789 organization and analysis of sequence data. *Bioinformatics* **28**, 1647–1649 (2012).
- 790 51. Martin, M. Cutadapt removes adapter sequences from high-throughput sequencing reads.
791 *EMBnet.journal* **17**, 10–12 (2011).
- 792 52. Schmieder, R. & Edwards, R. Quality control and preprocessing of metagenomic datasets.
793 *Bioinformatics* **27**, 863–864 (2011).
- 794 53. Langmead, B. & Salzberg, S. L. Fast gapped-read alignment with Bowtie 2. *Nat. Methods* **9**, 357–
795 359 (2012).
- 796 54. Katoh, K. & Standley, D. M. MAFFT multiple sequence alignment software version 7:
797 improvements in performance and usability. *Mol. Biol. Evol.* **30**, 772–780 (2013).
- 798 55. Guindon, S. & Gascuel, O. A simple, fast, and accurate algorithm to estimate large phylogenies by
799 maximum likelihood. *Syst. Biol.* **52**, 696–704 (2003).
- 800 56. Yang, Z. Maximum likelihood phylogenetic estimation from DNA sequences with variable rates
801 over sites: approximate methods. *J. Mol. Evol.* **39**, 306–314 (1994).
- 802 57. Darriba, D., Taboada, G. L., Doallo, R. & Posada, D. jModelTest 2: more models, new heuristics
803 and parallel computing. *Nat. Methods* **9**, 772 (2012).
- 804 58. Rambaut, A., Lam, T. T., Max Carvalho, L. & Pybus, O. G. Exploring the temporal structure of
805 heterochronous sequences using TempEst (formerly Path-O-Gen). *Virus Evol.* **2**, vew007 (2016).
- 806 59. Shapiro, B., Rambaut, A. & Drummond, A. J. Choosing appropriate substitution models for the

- 807 phylogenetic analysis of protein-coding sequences. *Mol. Biol. Evol.* **23**, 7–9 (2006).
- 808 60. Ferreira, M. A. R. & Suchard, M. A. Bayesian analysis of elapsed times in continuous-time Markov
809 chains. *The Canadian Journal of Statistics / La Revue Canadienne de Statistique* **36**, 355–368
810 (2008).
- 811 61. Baele, G. *et al.* Improving the accuracy of demographic and molecular clock model comparison
812 while accommodating phylogenetic uncertainty. *Mol. Biol. Evol.* **29**, 2157–2167 (2012).
- 813 62. Xie, W., Lewis, P. O., Fan, Y., Kuo, L. & Chen, M.-H. Improving marginal likelihood estimation for
814 Bayesian phylogenetic model selection. *Syst. Biol.* **60**, 150–160 (2011).
- 815 63. Gelman, A. & Meng, X.-L. Simulating Normalizing Constants: From Importance Sampling to
816 Bridge Sampling to Path Sampling. *Stat. Sci.* **13**, 163–185 (1998).
- 817 64. Drummond, A. J., Rambaut, A., Shapiro, B. & Pybus, O. G. Bayesian coalescent inference of past
818 population dynamics from molecular sequences. *Mol. Biol. Evol.* **22**, 1185–1192 (2005).
- 819 65. Churcher, T. S. *et al.* Public health. Measuring the path toward malaria elimination. *Science* **344**,
820 1230–1232 (2014).
- 821 66. Lloyd-Smith, J. O., Schreiber, S. J., Kopp, P. E. & Getz, W. M. Superspreading and the effect of
822 individual variation on disease emergence. *Nature* **438**, 355–359 (2005).
- 823 67. Nishiura, H., Yan, P., Sleeman, C. K. & Mode, C. J. Estimating the transmission potential of
824 supercritical processes based on the final size distribution of minor outbreaks. *J. Theor. Biol.* **294**,
825 48–55 (2012).
- 826 68. Perkins, T. A., Scott, T. W., Le Menach, A. & Smith, D. L. Heterogeneity, mixing, and the spatial
827 scales of mosquito-borne pathogen transmission. *PLoS Comput. Biol.* **9**, e1003327 (2013).
- 828 69. Kraemer, M. U. G. *et al.* Big city, small world: density, contact rates, and transmission of dengue
829 across Pakistan. *J. R. Soc. Interface* **12**, 20150468 (2015).
- 830 70. Kraemer, M. U. G. *et al.* Spread of yellow fever virus outbreak in Angola and the Democratic
831 Republic of the Congo 2015–16: a modelling study. *Lancet Infect. Dis.* **17**, 330–338 (2017/3).
- 832 71. Struchiner, C. J., Rocklöv, J., Wilder-Smith, A. & Massad, E. Increasing Dengue Incidence in

- 833 Singapore over the Past 40 Years: Population Growth, Climate and Mobility. *PLoS One* **10**,
834 e0136286 (2015).
- 835 72. Fauver, J. R. *et al.* Temporal and Spatial Variability of Entomological Risk Indices for West Nile
836 Virus Infection in Northern Colorado: 2006-2013. *J. Med. Entomol.* **53**, 425–434 (2016).
- 837 73. Rocklöv, J. *et al.* Assessing Seasonal Risks for the Introduction and Mosquito-borne Spread of Zika
838 Virus in Europe. *EBioMedicine* **9**, 250–256 (2016).
- 839 74. Ministry of Public Health, Ecuador. *National Direction of Epidemiological Surveillance for Vector*
840 *Transmitted Diseases (Spanish)* Available at: [http://www.salud.gob.ec/wp-](http://www.salud.gob.ec/wp-content/uploads/2015/12/GACETA-ZIKA_SE5corregido.pdf)
841 [content/uploads/2015/12/GACETA-ZIKA_SE5corregido.pdf](http://www.salud.gob.ec/wp-content/uploads/2015/12/GACETA-ZIKA_SE5corregido.pdf). (Accessed: 19th March 2017)
- 842 75. Zika Cumulative Cases. *Pan American Health Organization* Available at:
843 [http://www.paho.org/hq/index.php?option=com_content&view=article&id=12390&Itemid=42090&](http://www.paho.org/hq/index.php?option=com_content&view=article&id=12390&Itemid=42090&lang=en)
844 [ang=en](http://www.paho.org/hq/index.php?option=com_content&view=article&id=12390&Itemid=42090&lang=en). (Accessed: 1st December 2016)
- 845 76. Lessler, J. T. *et al.* Times to key events in the course of Zika infection and their implications: a
846 systematic review and pooled analysis. *Bull. World Health Organ.* (2016).
- 847 77. Lee, S. & Ramdeen, C. Cruise ship itineraries and occupancy rates. *Tourism Manage.* **34**, 236–237
848 (2013/2).
- 849 78. FCCA Research & Statistics. *Florida-Caribbean Cruise Association* Available at: [http://www.f-](http://www.fcca.com/research.html)
850 [cca.com/research.html](http://www.fcca.com/research.html). (Accessed: 1st March 2017)
- 851 79. Perkins, T. A., Siraj, A. S., Ruktanonchai, C. W., Kraemer, M. U. G. & Tatem, A. J. Model-based
852 projections of Zika virus infections in childbearing women in the Americas. *Nat Microbiol* **1**, 16126
853 (2016).
- 854 80. Hunter, J. D. Matplotlib: A 2D Graphics Environment. *Comput. Sci. Eng.* **9**, 90–95 (2007).

855

634 Extended Data

635 **Extended Data Fig. 1 | Miami-Dade mosquito surveillance and relative *Aedes aegypti* abundance.** (a)
636 Mosquito surveillance data reported from June 21 to November 28, 2016 was used to evaluate the risk of
637 ZIKV infection from mosquito-borne transmission in Miami. A total of 24,306 *Ae. aegypti* and 45 *Ae.*
638 *albopictus* were collected. Trap nights are the total number of times each trap site was used and the trap
639 locations are shown in Fig. 1d (some “Other Miami” trap sites are located outside of mapped region). Up
640 to 50 mosquitoes of the same species and trap night were pooled together for ZIKV RNA testing. The
641 infection rates were calculated using a maximum likelihood estimate (MLE). None of the *Ae. albopictus*
642 pools contained ZIKV RNA. (b) The number of weekly ZIKV cases (based on symptoms onset) was
643 correlated with mean *Ae. aegypti* abundance per trap night determined from the same week and zone
644 (Spearman $r = 0.61$). This suggests that when the virus is present, mosquito abundance numbers alone
645 could be used to target control efforts. (c) Insecticide usage, including truck and aerial adulticides and
646 larvacides, by the Miami-Dade Mosquito Control in Wynwood (left) and Miami Beach (right) was
647 overlaid with *Ae. aegypti* abundance per trap night to demonstrate that intense usage of insecticides may
648 have helped to reduce local mosquito populations. (d) Relative *Ae. aegypti* abundance for each Florida
649 county and month was estimated using a multivariate regression model, demonstrating spatial and
650 temporal heterogeneity for the risk of ZIKV infection.

651
652 **Extended Data Fig. 2 | Maximum likelihood tree and root-to-tip regression of Zika virus genomes**
653 **from Pacific islands and the epidemic in Americas.** (a) Maximum likelihood tree of publicly available
654 ZIKV sequences and sequences generated in this study ($n=104$). tips are coloured by location, labels in
655 bold indicate sequences generated in this study, Florida clusters F1-F4 are indicated by vertical lines to
656 the right of the tree. Bootstrap support values are shown at key nodes. All other support values can be
657 found in Supplementary File 1. (b) Linear regression of sample tip dates against divergence from root
658 based on sequences with known collection dates estimates an evolutionary rate for the ZIKV phylogeny
659 of 1.10×10^{-3} nucleotide substitutions/site/year (subs/site/yr). This is consistent with BEAST analyses
660 using a relaxed molecular clock and a Bayesian Skyline tree prior, the best-performing combination of
661 clock and demographic model according to marginal likelihood estimates (Extended Data Table 1c),
662 which estimated an evolutionary rate of 1.21×10^{-3} (95% highest posterior density: $1.01 - 1.43 \times 10^{-3}$)
663 subs/site/yr (Extended Data Table 1a). These values are in agreement with previous estimates calculated
664 based on ZIKV genomes from Brazil⁶.

665
666 **Extended Data Fig. 3 | Molecular clock dating of Zika virus clades.** Maximum clade credibility
667 (MCC) tree of ZIKV genomes collected from Pacific islands and the epidemic in Americas ($n=104$).
668 Circles at the tips are colored based on origin location. Clade posterior probabilities are indicated by
669 white circles filled with black relative to the support. A posterior probability of 1 fills the entire circle
670 black. The grey violin plot indicates the 95% highest posterior density (HPD) interval for the tMRCA of
671 the American epidemic. We estimated that the tMRCA for the ongoing epidemic in the Americas
672 occurred during October, 2013 (node AM, Extended Table 1, 95% HPD: August, 2013-January, 2014),
673 which is consistent with previous analysis based on ZIKV genomes from Brazil⁶.

674
675 **Extended Data Fig. 4 | Estimation of basic reproductive number and number of introductions in**
676 **Miami-Dade County.** (a) Probability distribution of estimated total number of cases caused by a single
677 introduction (excluding the index case) for different values of R_0 . (b) Mean and 95% CI for total number
678 of local cases caused by 320 introduction events (*i.e.*, travel-associated cases diagnosed in Miami-Dade
679 County) for different values of R_0 and for different assumptions of proportion of infectious travelers. (c)
680 Log likelihood of observing 241 local cases in Miami-Dade County with 320 introduction events for
681 different values of R_0 along with 95% maximum likelihood estimate (MLE) bounds on R_0 . (d) Mean and
682 95% uncertainty interval for total number of distinct phylogenetic clusters observed in 27 sequenced
683 ZIKV genomes from human cases diagnosed in Miami-Dade County for different values of R_0 and for

684 different assumptions of sampling bias, from $\alpha=1$ (no sampling bias) to $\alpha=2$ (skewed toward
685 preferentially sampling larger clusters). (e) Log likelihood of observing 3 clusters (*i.e.*, ZIKV lineages F1,
686 F2, and F4, Fig. 2a) in 27 sequenced cases for different values of R_0 along with 95% MLE bounds on R_0 .
687 (f) Mean and 95% CI for total number of local cases caused by 320 observed travel-associated cases with
688 travel-associated vs local reporting rates of 50%/25% and 10%/5%. This assumes 50% of travelers are
689 infectious. (g) Log likelihood of observing 241 local cases with 320 introduction events for different
690 values of R_0 along with 95% MLE bounds on R_0 with travel-associated vs local reporting rates of
691 50%/25% and 10%/5%. (h) Mean and 95% uncertainty interval for total number of distinct phylogenetic
692 clusters observed in 27 sequenced ZIKV genomes for different values of R_0 and for assumptions of local
693 reporting rate of 5% and 25%. This assumes preferential sampling ($\alpha=2$). (i) Log likelihood of observing
694 3 clusters in 27 sequenced cases for different values of R_0 along with 95% MLE bounds on R_0 with local
695 reporting rate of 5% and 25%. At 5% local reporting rate, 0 of the 100,000 replicates for all R_0 values
696 showed 3 clusters.

697

698 **Extended Data Fig. 5 | Weekly reported Zika virus case numbers and incidence rates in the**
699 **Americas.** (a) Most ZIKV case numbers reported by PAHO³⁰ were only available as bar graphs (raw data
700 was not made available to us at the time of request). Therefore we used the WebPlotDigitizer to estimate
701 the weekly case numbers from the PAHO bar graphs. ZIKV cases reported from Ecuador was the only
702 data set to include a link to the actual case numbers that also had >10 cases per week⁷⁴. To validate the
703 WebPlotDigitizer, we compared the weekly reported case numbers from Ecuador to our estimates. (b)
704 The reported and estimated case numbers were strongly correlated (Spearman $r = 0.9981$). The
705 WebPlotDigitizer was used to estimate the ZIKV case numbers for all subsequent analysis. (c) ZIKV
706 cases (suspected and confirmed) and (d) incidence rates (normalized per 100,000 population) are shown
707 for each country or territory with available data per epidemiological week from January 1 to September
708 18, 2016. (e) Each country or territory with available data is colored by its reported ZIKV incidence rate
709 from January to June, 2016 (the time frame for analysis of ZIKV introductions into Florida).

710

711 **Extended Data Fig. 6 | Cruise and flight traffic entering Miami from regions with Zika virus**
712 **transmission.** The estimated number of passengers entering Miami, by either (a) cruises or (b) flights,
713 from each country or territory in the Americas with ZIKV transmission per month (left panel). The center
714 map and inset show the cumulative numbers of travelers entering Miami during January to June, 2016
715 (the time frame for analysis of ZIKV introductions into Florida) from each country or territory per method
716 of travel. (c) The total traffic (*i.e.* cruises and flights) is shown entering Miami per month.

717

718 **Extended Data Fig. 7 | Expected number of Zika virus infected travelers from the Caribbean is**
719 **correlated with the total observed number of travel-associated infections.** (a) In order to account for
720 potential biases in ZIKV reporting accuracies, we also estimated the proportion of infected travelers using
721 projected ZIKV attack rates⁷⁹ (*i.e.* predicted proportion of population infected before epidemic burnout).
722 About 60% of the infected travelers are expected to have arrived from the Caribbean, similar to our
723 results using incidence rates (Fig. 3c). (b) The expected number of travel-associated ZIKV cases were
724 estimated by the number of travelers coming into Miami from each country/territory (travel capacity) and
725 the in-country/territory infection likelihood (incidence rate per person) per week. The expected travel
726 cases were summed from all of the Americas (left), Caribbean (left center), South America (right center),
727 and Central America (right) and plotted with the observed travel-associated ZIKV cases. Numbers in each
728 plot indicate Spearman correlation coefficients. Negative Spearman r coefficients indicated a negative
729 correlation between the number of expected and observed travel cases.

730

731 **Extended Data Fig. 8 | Greater early season potential for Zika virus introductions into Miami.** The
732 monthly cruise ship and airline²⁸ capacity from countries/territories with ZIKV transmission for the major
733 United States travel hubs (shown as circle diameter) with monthly potential *Ae. aegypti* abundance (circle
734 color), as previously estimated²². The abundance ranges were chosen with respect to the May-Oct Miami

735 mean: “None to low” (<2%), “Low to moderate” (2-25%), “Moderate to high (25-75%), and “High”
736 (>75%). Mosquito-borne transmission is unlikely in the “None to low” range. Cruise capacities from
737 Houston and Galveston, Texas were combined.

738

739 **Extended Data Table 1 | (a) Time of the most recent common ancestor and evolutionary rate and**
740 **(b) Model selection to infer time-structured phylogenies.**

741 HPD, highest posterior density. Dates listed as proportion of days elapsed with a year. Clades refer to Fig.
742 2a.

743

744 **Extended Data Table 2 | Validation of sequencing results.**

745 ^a Compared to the consensus genomes generated by sequencing 35 × 400 bp amplicons on the MiSeq.

746 ^b Amplicons produced using Ion AmpliSeq and 875 custom ZIKV primers.

747 NGS, next-generation sequencing; UTR, untranslated region; CDS, coding sequence.

748

749

750

751

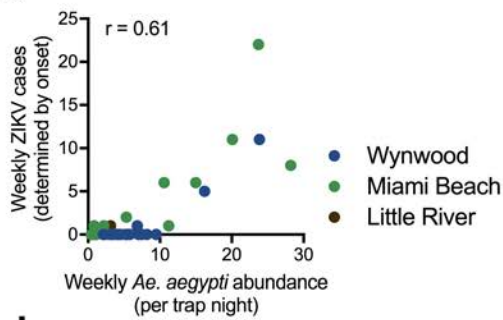
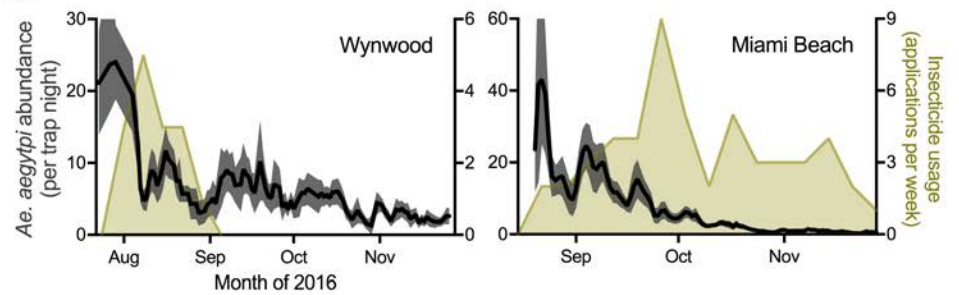
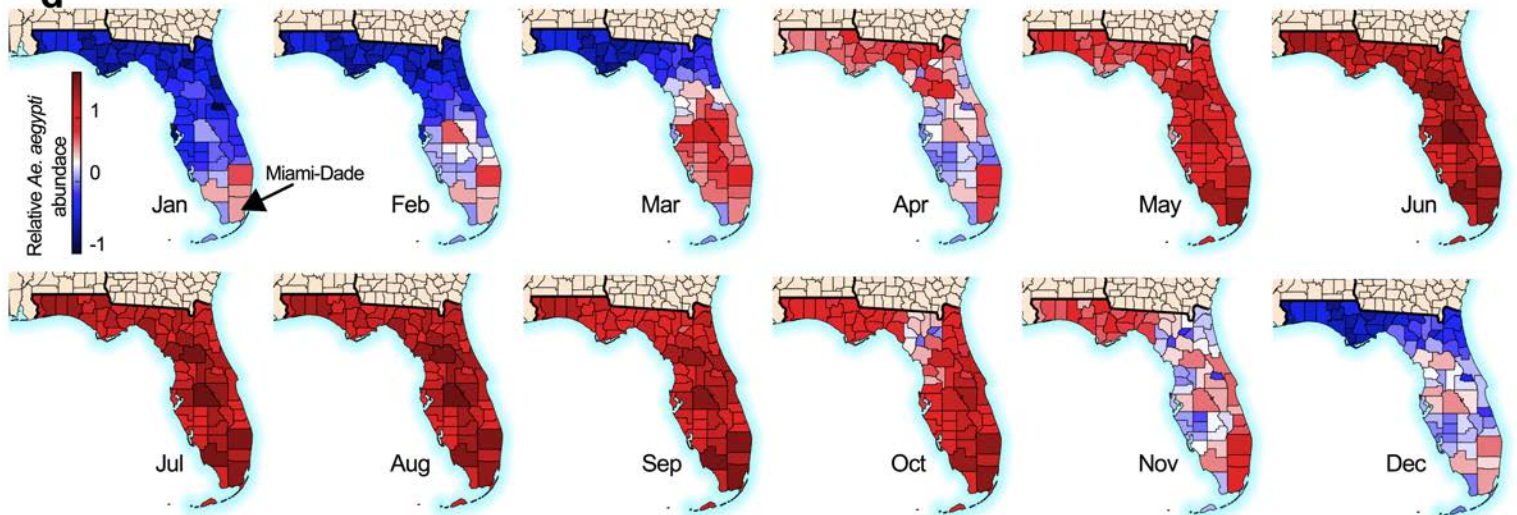
752

753

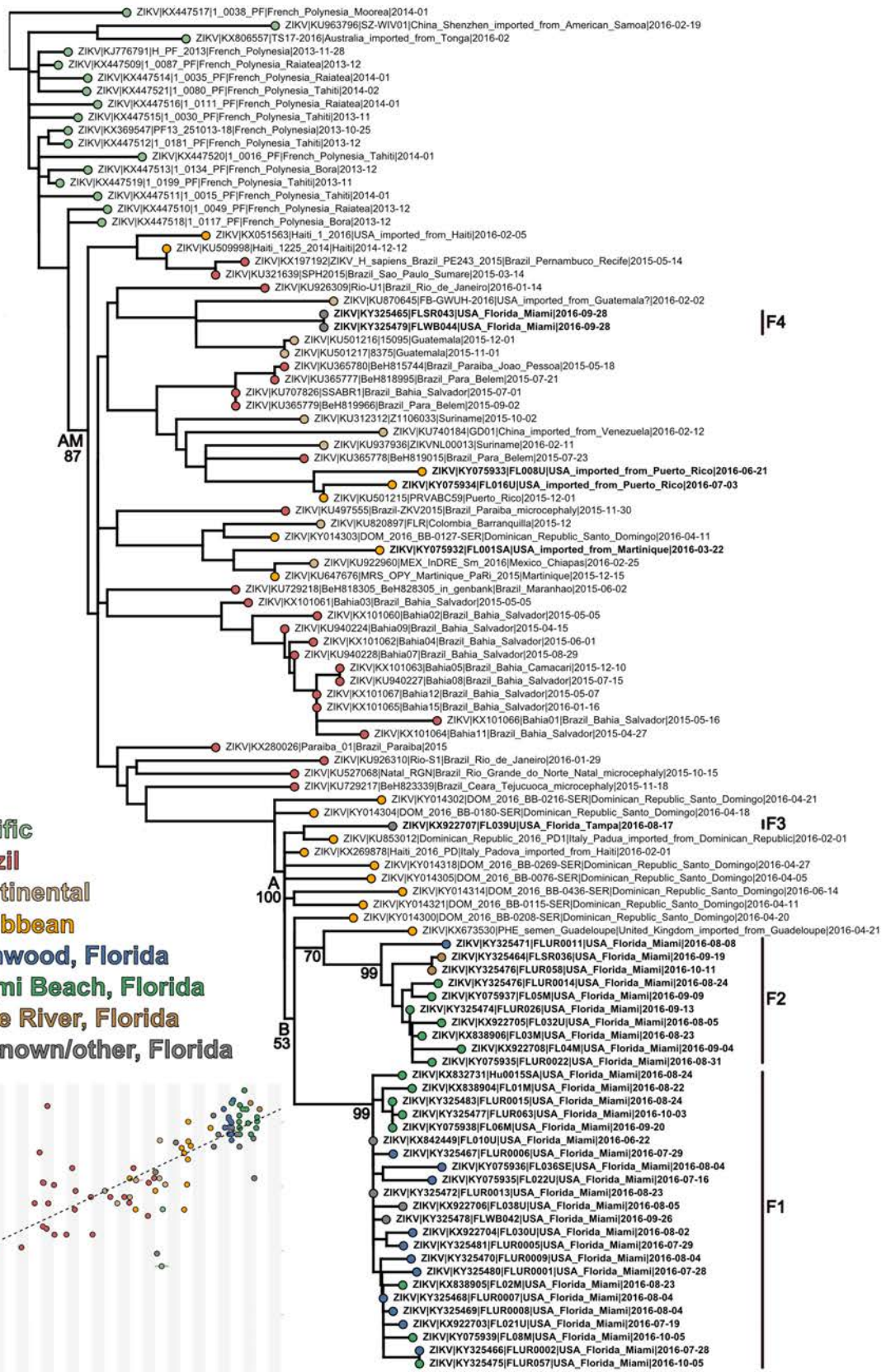
754

a**Miami-Dade mosquito surveillance**

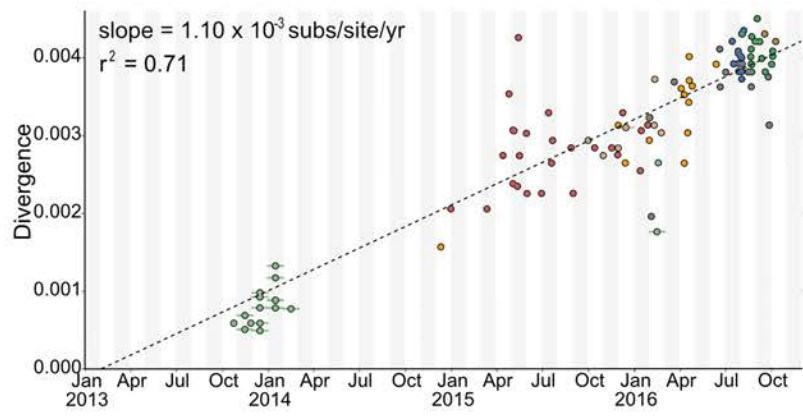
Location	Start date	End date	Trap sites	Trap nights	<i>Ae. aegypti</i> collected	No. per trap night	Pools tested	ZIKV+ pools	MLE infection rate
Wynwood	Jul 23	Nov 25	29	824	4,972	6.0	738	0	0
Miami Beach	Aug 21	Nov 28	29	2,180	13,265	6.1	1,473	8	0.61 (0.28-1.15)
Little River	Oct 15	Nov 28	5	217	485	2.2	136	0	0
Other Miami	Jun 21	Sep 23	52	235	5,584	23.8	249	0	0

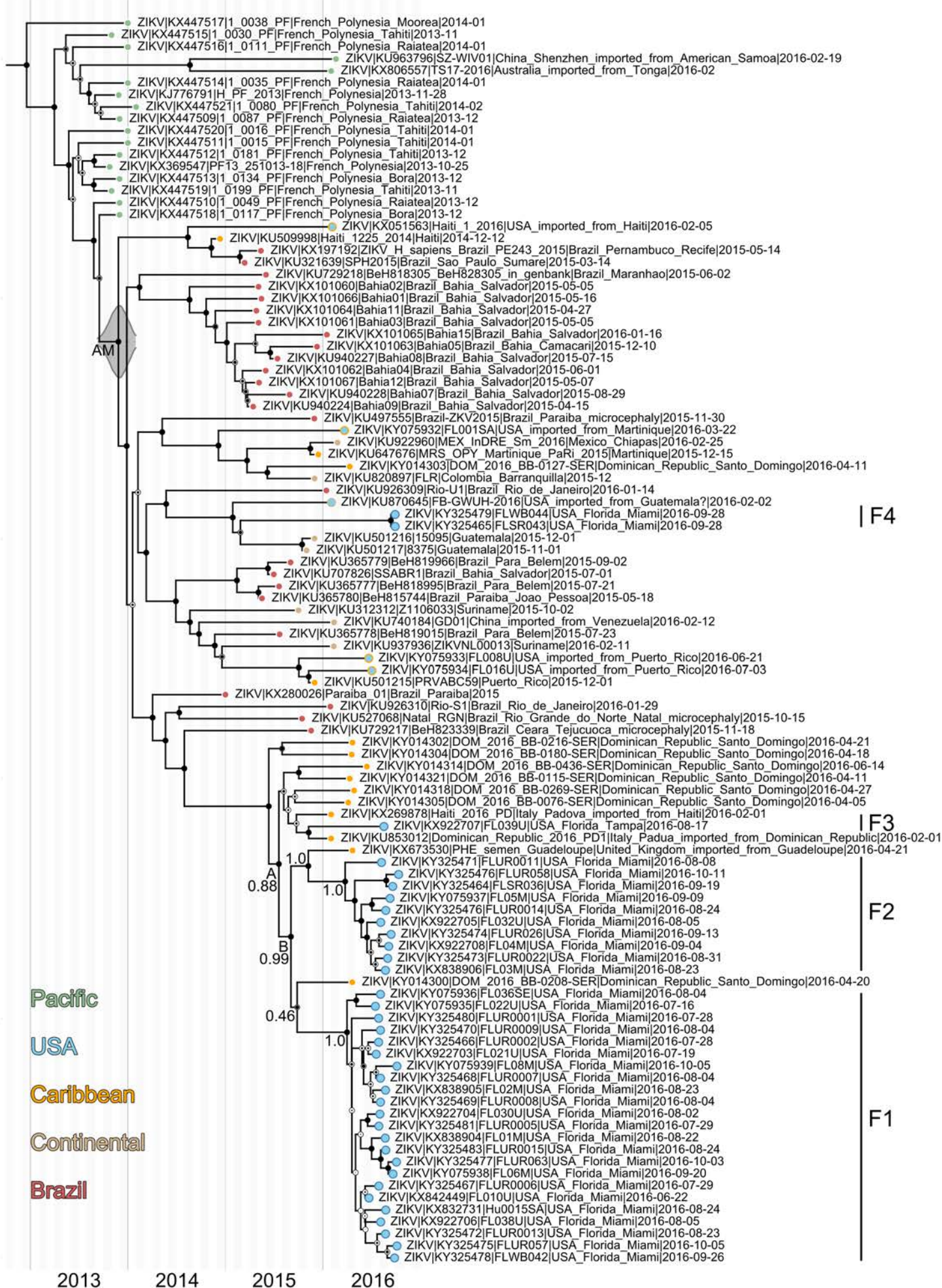
b**c****d**

a



b





Pacific
 USA
 Caribbean
 Continental
 Brazil

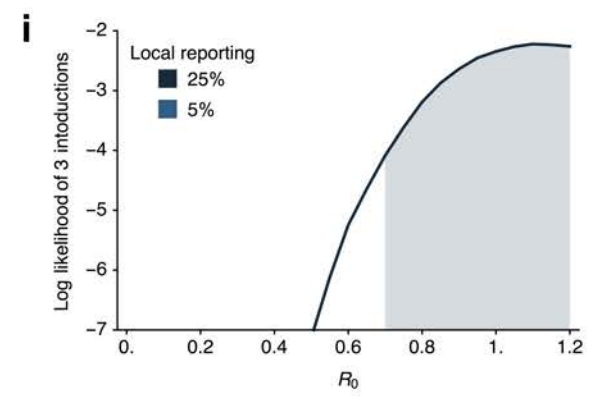
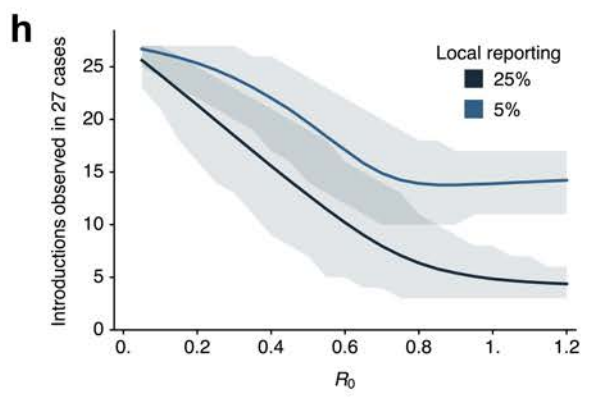
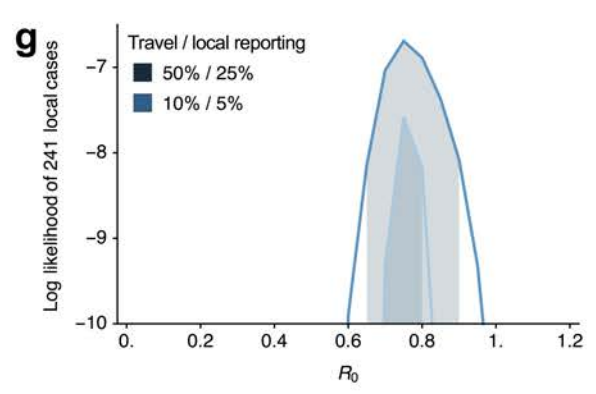
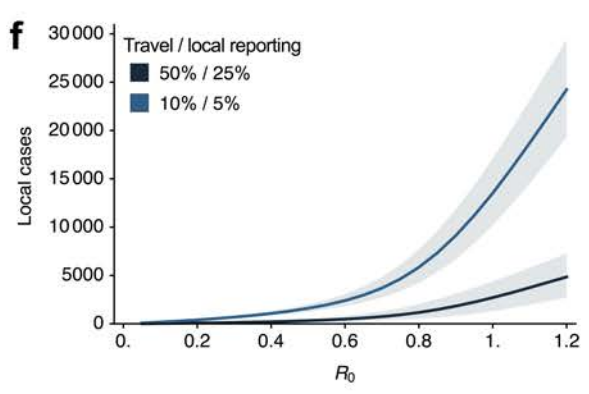
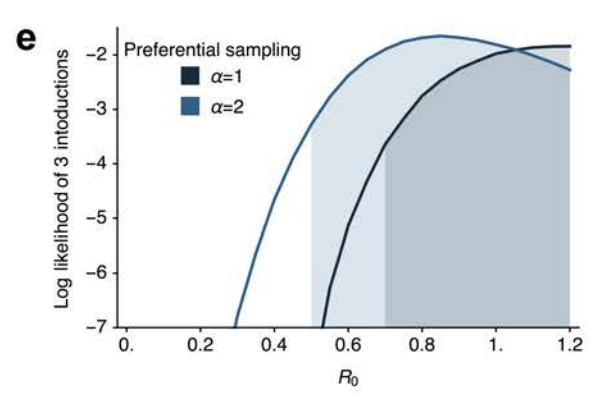
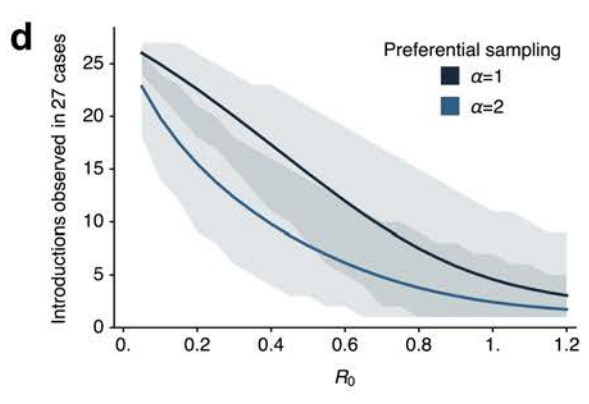
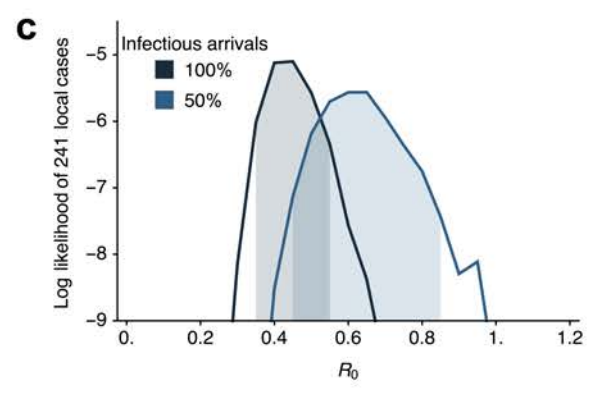
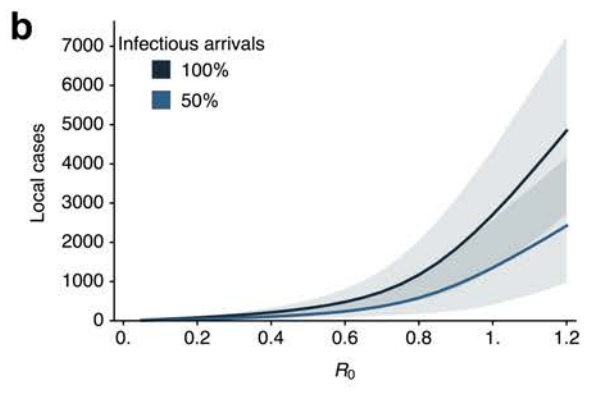
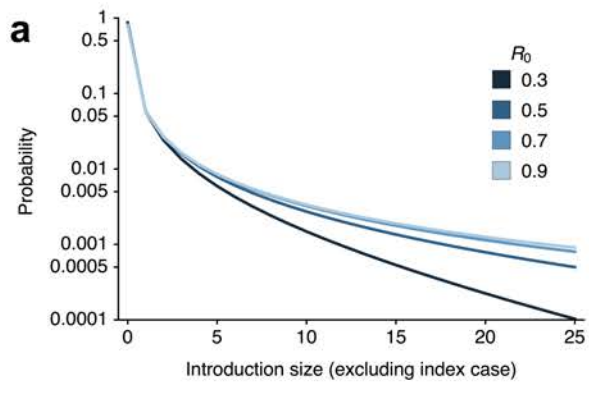
F4

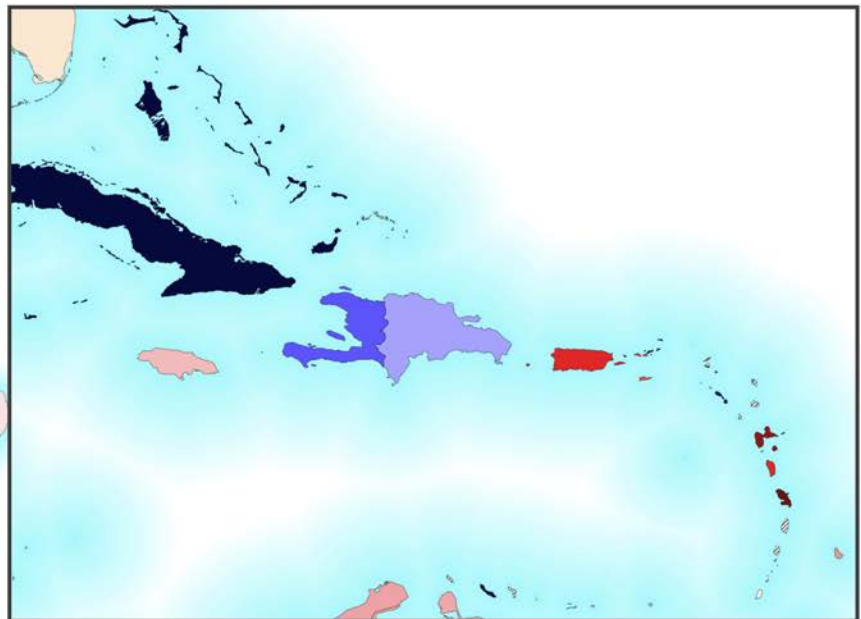
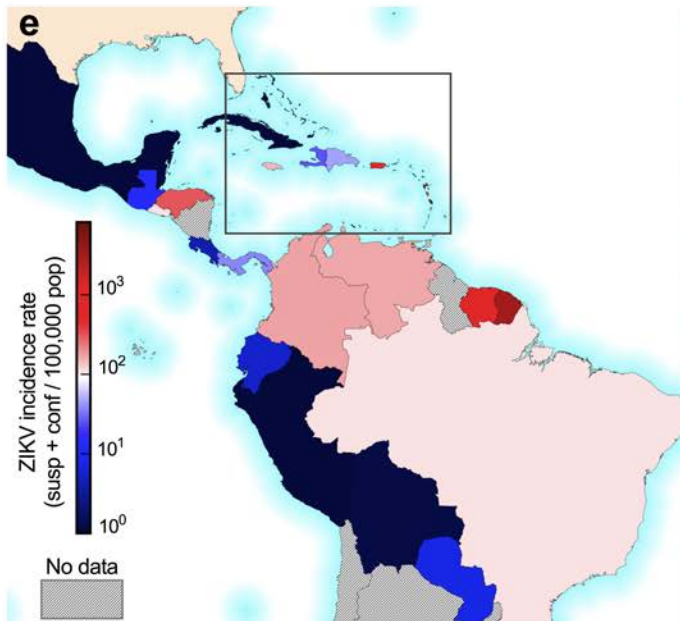
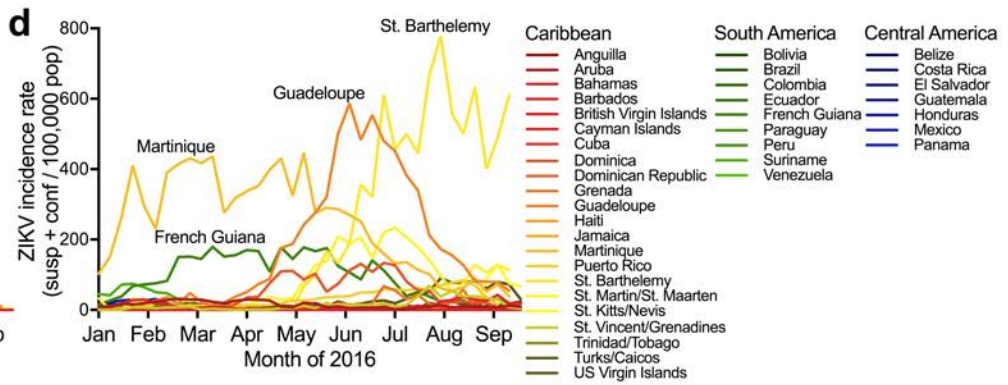
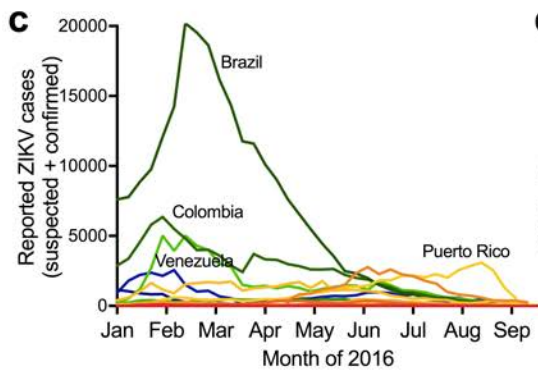
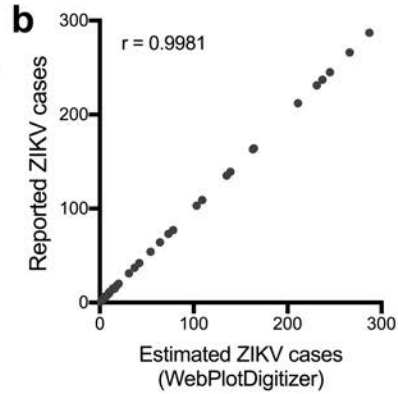
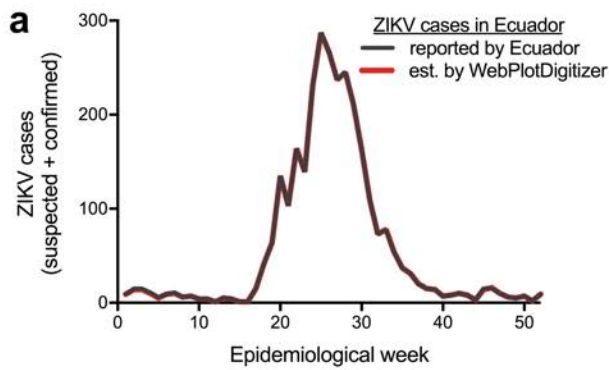
F3

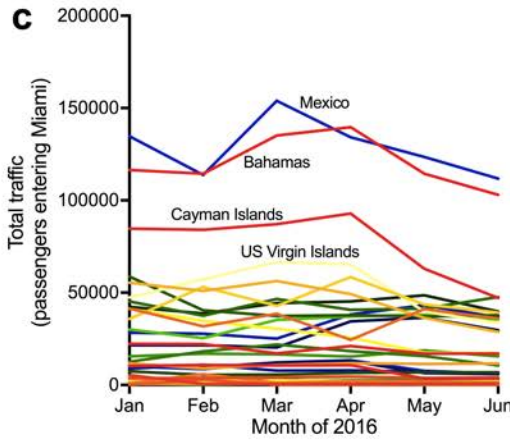
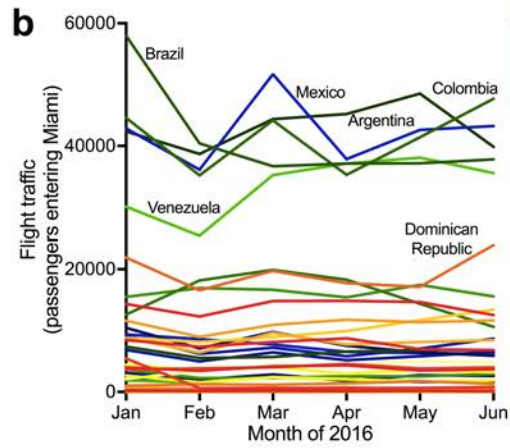
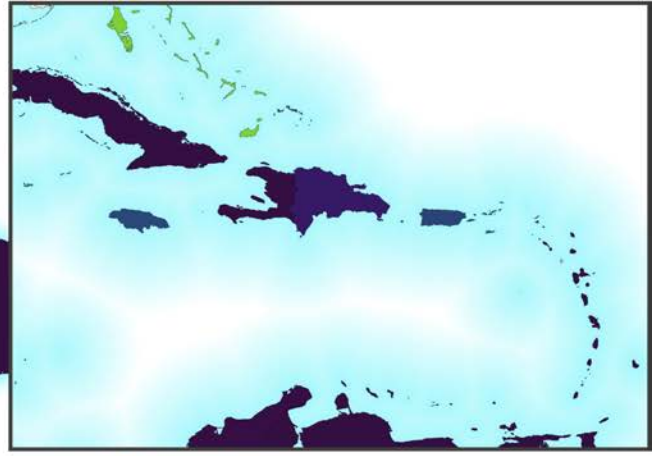
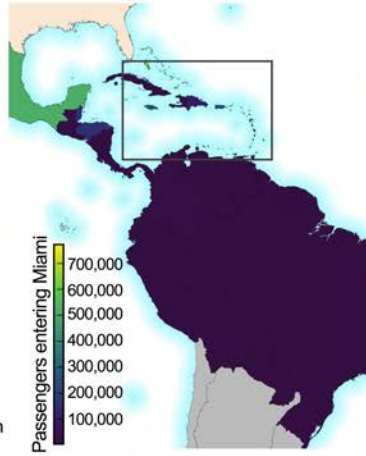
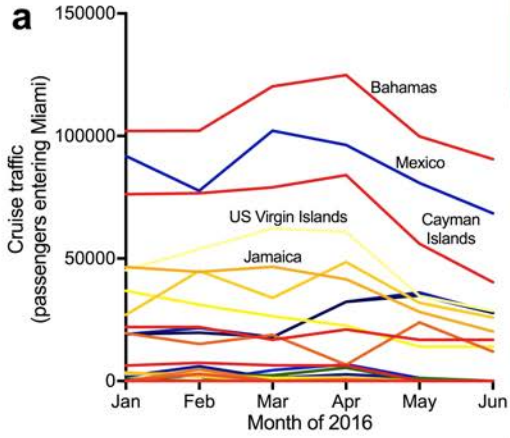
F2

F1

2013 2014 2015 2016







- | Caribbean | South America | Central America |
|------------------------|---------------|-----------------|
| Bahamas | Argentina | Belize |
| Barbados | Bolivia | Costa Rica |
| British Virgin Islands | Brazil | El Salvador |
| Cayman Islands | Colombia | Guatemala |
| Cuba | Ecuador | Honduras |
| Curacao | French Guiana | Mexico |
| Dominica | Paraguay | Panama |
| Dominican Republic | Peru | |
| Grenada | Suriname | |
| Guadeloupe | Venezuela | |
| Haiti | | |
| Jamaica | | |
| Martinique | | |
| Puerto Rico | | |
| St. Barthelemy | | |
| St. Martin/St. Maarten | | |
| St. Kitts/Nevis | | |
| US Virgin Islands | | |

